THESIS WORK FOR DUAL MASTER'S DEGREE

ITBA Mag. in Energy and Environment

KIT M.Sc. in Mechanical Engineering

OPTIMIZATION OF THE ORGANIC RANKINE CYCLE POWER PLANT MONIKA'S CONTROL SYSTEM

Juan Francisco Gutiérrez Guerra

Chemical Engineer
Instituto Tecnológico de Buenos Aires

Tutor
Dipl. Ing. Hans-Joachim Wiemer, KIT/ITES

Co-Tutor
Dr. Nicolás Nemirovsky, ITBA

Examiner
Prof. Dr.-Ing. Andreas Class , KIT/ITES

Karlsruhe
08/02/2021

Verfassererklärung

Ich versichere wahrheitsgemäß, die Arbeit selbstständig verfasst, alle benutzten Hilfsmittel vollständig und genau angegeben und alles kenntlich gemacht zu haben, was aus Arbeiten anderer unverändert oder mit Abänderungen entnommen wurde sowie die Satzung des KIT zur Sicherung guter wissenschaftlicher Praxis in der jeweils gültigen Fassung beachtet zu haben.

Datum Unterschrift

Acknowledgement

I would like to express my gratitude to the people who guided and supported me throughout the time I have been working in this Thesis, whose encouragement and inspiration allowed me to conclude another step in my professional life in times of adversity.

To Dr. Cecilia Smoglie.

To my Thesis directors at KIT, Dipl. Ing. Hans-Joachim Wiemer and Prof. Dr.-Ing. Andreas Class, as well as my Thesis advisor at ITBA, Dr. Nicolás Nemirovsky.

To my colleagues, Federico Wagner, Macarena Alvarez, Eugenio Torres de Ritter, Luciano Gardella and Mariano Fossati.

And most especially, to my family and friends.

Abstract

The aim of this work was to optimize the MoNiKa organic Rankine cycle power plant control system. In particular, performance and robustness of the PID control loops were evaluated for the main and support feed pumps and throttling valve. Each component was physically modelled in Simscape, while control simulations were performed in Simulink based on process transfer functions. The tuning methods were chosen in order to achieve faster, more robust responses to setpoint and disturbances changes. Stability, sensitivity and settling time values were calculated on MATLAB based on frequency response techniques, and results were compared with a set of previously measured data. Final results showed that, using the Continuous Cycling Method, the optimized controllers' parameters were able to provide a better setpoint tracking and disturbance rejection, while accomplishing up to 10 times faster responses than the preliminary PID controllers' settings.

Resumen

El objetivo de este trabajo fue optimizar el sistema de control del ciclo orgánico Rankine de potencia MoNiKa. En particular, se evaluó el desempeño y robustez de los lazos de control PID de las bombas principal y de soporte y de la válvula de estrangulación. Los componentes fueron modelados en Simscape, mientras que las simulaciones de los sistemas de control se ejecutaron en Simulink, en base a funciones de transferencia. Los métodos de ajuste fueron seleccionados para brindar respuestas más rápidas y robustas ante cambios de setpoint y perturbaciones. Valores de estabilidad, sensibilidad y tiempo de asentamiento fueron calculados en MATLAB en base a técnicas de respuesta en frecuencia, y los resultados fueron comparados con un conjunto de mediciones previamente tomadas. Los resultados finales demostraron que, usando el Método de Ciclo Continuo, los parámetros optimizados lograron un mejor seguimiento de setpoint, mejor rechazo a perturbaciones y respuestas hasta 10 veces más rápidas que los parámetros preliminares.

Zussamenfassung

Ziel dieser Arbeit war die Optimierung des Regelsystems des MoNiKa Organic Rankine Cycle Kraftwerks. Insbesondere wurden die Leistung und die Robustheit der PID-Regelkreise für die Haupt- und Hilfsspeisepumpen und das Drosselventil bewertet. Jede Komponente wurde in Simscape physikalisch modelliert, während die Regelungssimulationen in Simulink auf der Grundlage von Prozessübertragungsfunktionen durchgeführt wurden. Die Verfahren zur Bestimmung von Reglerparametern wurden gewählt, um schnellere und robustere Reaktionen auf Sollwert- und Störungsänderungen zu erzielen. Die Werte für Stabilität, Empfindlichkeit und Einschwingzeit wurden mit MATLAB auf der Grundlage von Frequenzgangtechniken berechnet, und die Ergebnisse wurden mit einer Reihe von zuvor gemessenen Daten verglichen. Die Endergebnisse zeigten, dass die optimierten Reglerparameter unter Verwendung der Continuous Cycling Ziegler-Nichols Methode in der Lage waren, eine bessere Sollwertnachführung und Störungsunterdrückung zu gewährleisten und gleichzeitig bis zu 10-mal schneller zu reagieren als die vorläufigen PID-Reglereinstellungen.

Index

List of abbreviations and symbols

ORC	Organic Rankine Cycle	SP	Setpoint
MoNiKa	Modular Low Temperature Cycle Karlsruhe	TF	Transfer function
s	Complex Laplace variable	G_{OL}	Open-loop transfer functiom
z	Discrete time parametrization symbol	Gc	Controller transfer function
Ysp	Setpoint signal	Ga	Actuator transfer function
E	Error signal	Gp	Process transfer function
P	Controller Output	Gd	Disturbance transfer function
U	Manipulated Variable	Gm	Transmitter transfer function
Y	Controlled Variable	SSTR	Summer semester test run's parameters
D	Disturbance Variable	ZN	Ziegler-Nichols controller parameters
Ym	Measured value of Y	TL	Tyreus-Luyben controller parameters
Yu	Change in Y due to U	S	Sensitivity function
Yd	Change in Y due to D	T	Complementary sensitivity function

K_v	Valve's flow factor	$m^3/h.bar^{0.5}$	GAIN	MoNiKa's proportional gain	-
K_{v_s}	Kv value at maximum flow	$m^3/h.bar^{0.5}$	TN	MoNiKa's integral gain	s
$\dot{m_{ORC}}$/m	Propane's mass flow	kg/h / kg/s	TD	MoNiKa's derivative gain	s
ρ	Density	kg/m^3	T1	MoNiKa's filter coefficient	s
SG_{in}	Inlet specific gravity	-	Kcu	Ultimate gain	-
ΔP/dp	Pressure difference	bar / MPa	Pu	Ultimate period	rad/s
p In	Inlet pressure	bar / MPa	ωc	Critical frequency	rad/s
p Out	Outlet pressure	bar / MPa	GM	Gain margin	-
RAF	Rotation angle fraction	%	PM	Phase margin	deg
ts	Sample time	s	ARc	Gain crossover frequency	rad/s
P	Proportional gain	-	Φ_g	Phase angle at ARc	deg
I	Integral gain	1/s	M_T	T's amplitude ratio	-
D	Derivative gain	s	M_S	S's amplitude ratio	-
N	Derivative filter coefficient	1/s	BW	Bandwidth	rad/s

1 Introduction

1.1 Geothermal Energy and Organic Rankine Cycles

In a context characterized by the increasing energy demand and the determination of preventing global warming from increasing at higher levels, efforts are put on finding energy resources which could substantially reduce carbon dioxide and other greenhouse gases emissions. As a result, renewable energy systems continue to become more efficient, while their share of total energy consumption increases.

Beneath the Earth's surface, geothermal reservoirs contain water streams at different levels of high temperatures and pressures. The use of these hot water and vapor streams for heating or electricity generation purposes, among others uses, is known as geothermal energy. Since the water is generally reinjected to the Earth after being used, it is considered a sustainable, clean, and renewable resource.

In regard to electricity generation, three main categories of geothermal power plants can be considered, depending on temperature, pressure, and chemistry of the thermal resource: condensing power plants, with dry steam and single or double flash systems; back-pressure turbines, which exhaust steam at above atmospheric pressures; and binary cycle power plants, which user lower-temperature water (~150°C) [1].

The improvement in drilling technology and the development of binary plants have enabled enhanced geothermal systems in diverse areas containing low-enthalpy reservoirs. Electricity generation in this type of plants is usually done using an Organic Rankine Cycle.

ORC processes use organic fluids with lower boiling points than the water liquid-vapor phase change, thus making possible for the cycle to provide useful work from low-enthalpy heat resources.

The main components of an ORC are schematized in Figure 1. As in any Rankine cycle, the liquid working fluid is pumped into a heat exchanger, where evaporation takes place. In this case, heat is provided by a low-temperature geothermal water stream, which is reinjected into a well once it is cooled. The dry, saturated organic fluid is then expanded through a turbine, converting useful work into electrical energy. As pressure and temperature decrease, the resulting wet vapor is cooled in a condenser, where the vapor-liquid phase change occurs, before passing through the feed pump, where the cycle restarts. Air is generally used as cooling fluid.

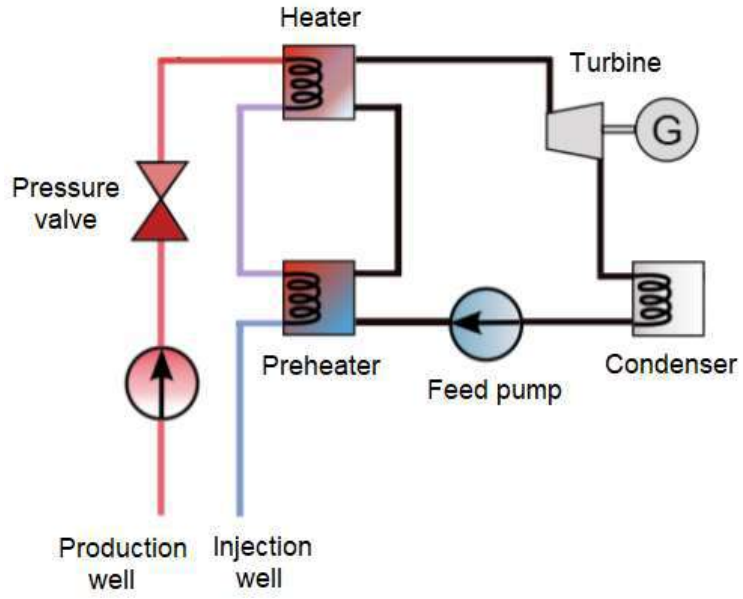

***Figure 1**: Main components of an ORC power plant with geothermal application*

Selection of a suitable working fluid has a major influence on the overall cycle performance. Ideally, a fluid with high stability and heat of vaporization is preferably used. Saturation vapor curve characteristics and variables such as availability, safety and environmental impact are also considered at the moment of selecting the organic fluid [2].

1.2 MoNiKa Power Plant

MoNiKa (Modular Low Temperature Cycle Karlsruhe), is a small, modular, mobile installation consisting of an ORC power plant. Located in the Karlsruhe Institute of Technology North Campus, and run by the Institute of Thermal Energy Technology and Safety (ITES), the installation facilitates the study and research of low-temperature power generation from low-enthalpy thermal resources.

Each main component of the power plant is interchangeable. A synthetic thermal water stream, which is emulated by a flow of hot water heated up by a boiler, works as the binary cycle's hot source. These features give the installation the flexibility to allow different arrangements and boundary conditions [3].

Previous research works show that, compared to subcritical processes with other organic fluids, a higher performance can be achieved using propane as working fluid: cycles using propane with supercritical vapor can achieve a specific net power output of 36.8 kWs/kg, and a thermal efficiency of 10.1% [4]. Thus, MoNiKa's ORC is a supercritical process and uses propane as working fluid. Its full load point is designed for a thermal power of ~1000 kW, with live steam design parameters of 5.5 MPa and 117°C at the turbine inlet.

First measurements were carried out during Winter Semester 2019, and the results are discussed in Luciano Gardella's Master Thesis Work [5]. Test runs were performed in a quasi-stationary regime and bypass configuration, meaning that the expansion of the working fluid took place in a throttling valve, instead of the turbine. The operation was manually done, and three part loads were studied (100%, 70%, and 50% ORC mass flow). In full load operation, live steam parameters of 5.5 MPa and 108°C were achieved at the throttling valve inlet, being 2.9 kg/s the ORC mass flow and maintaining constant the waterside conditions.

The results obtained in this work, together with a second set of measurements carried out by ITES during Summer Semester 2020, compose the data used for validation purposes in this present work. The Summer Semester hot runs were carried out not manually, but with the control system already working with preliminary controllers' settings. All measured data is presented in the Appendix Section.

1.2.1 Components Description

A schematic diagram for the power plant in the bypass configuration is presented in Figure 2. Expansion of the working fluid happens in the throttling valve instead of the turbine. The bypass valves, which open the way for the propane to flow across the throttling valve, are not involved in the scope of this work.

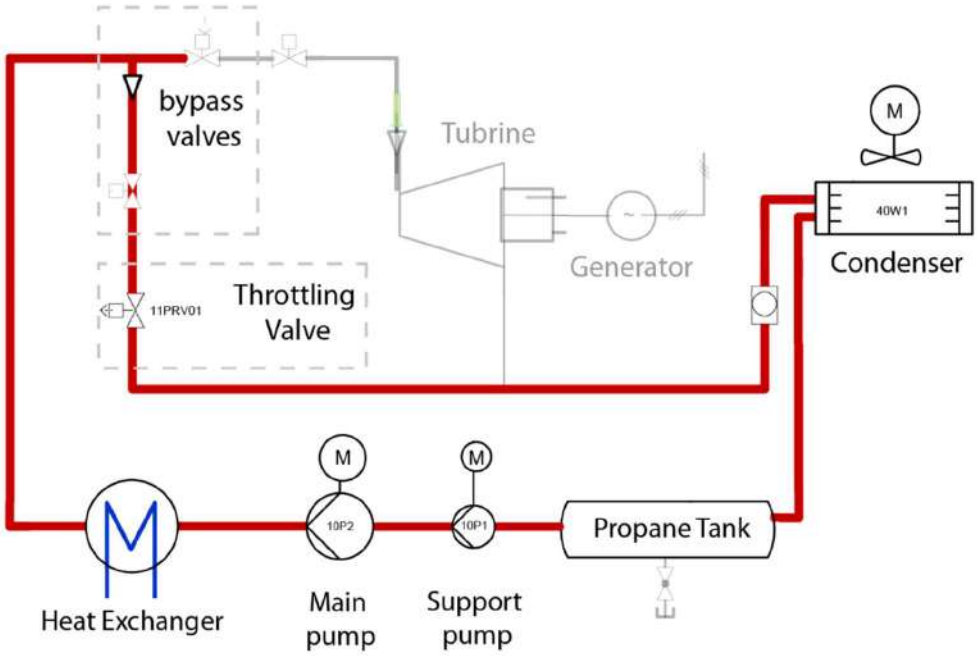

***Figure 2**: MoNiKa's bypass configuration schematic diagram*

Because the aim is to optimize the control loops involving the pumping system and the throttling valve, a description of only these components is presented in the following sections.

1.2.1.1 Pumping System

The system is composed of two pumps. On the one hand, a 5.5kW GRUNDFOS vertical, multistage centrifugal pump, from now on referred as support pump, had to be installed to provide the saturated propane flowing from the tank, the necessary pressure head (0.05 MPa) to prevent cavitation in the main pump. Rotational energy is given by a 3-phase, fan cooled asynchronous motor. Its main technical information is presented in Table 1 [6]:

Description	Value
Product Name	CRN 20-4 A-FGJ-H-E-HQQE
Max head	2.883 bar
Rated head	2.29 bar
Rated flow	21000 l/h
Rated speed	2920 rpm
Stages	4
Impeller	4
Max. operating pressure	25 bar
Electrical data	
Rated power	5.5 kW
Mains frequency	50 Hz
Motor efficiency at full load	89.2%

***Table 1**: Support pump technical data*

On the other hand, a LEWA triple diaphragm pump, from now on referred as main pump, provides the working fluid the necessary head to achieve the live steam pressure (5.5 MPa) at high efficiencies, independently of the mass flow. Rotational energy is also given by an asynchronous motor. Its main technical information is presented in Table 2 [7]:

Description	Value
Drive Unit	G3G
Pump head type	M514US
Plunger diameter	100 mm
Max stroke frequency	160 spm
Gear reduction (rpm/spm)	10.25
Max flow rate	26260 l/h
Displacement	0.260 l/rev
Max permissible working pressure	62 bar
Rod force	60 kN
Electrical data	
Rated power	75 kW
Mains frequency	50 Hz
Rotational speed	1470 rpm

***Table 2**: Main pump technical data*

Both manufacturers provide all the performance curves needed to define the different operation points. In the case of the support pump, mass flow, pressure difference, (and density) are required to define the pump speed. For the main pump, however, only mass flow (and density) is needed.

1.2.1.2 Throttling Valve

A rotary plug VETEC control valve works as the expansion element in the current configuration of the power plant. Its body is made of stainless cast and carbon steel and has a design temperature range of -20 to 130°C.

An electro-pneumatic positioner with PROFIBUS-PA communication is attached to the valve and is used to assign the valve position to the control signal. The natural characteristic of the rotary plug valve is designed to follow an equal-percentage behavior. Both curves, natural and equal-percentage characteristics, are provided by the manufacturer (Figure 3). Given the Kv% value calculated in the valve inlet (1.1), the rotation angle fraction can be defined using these curves [8].

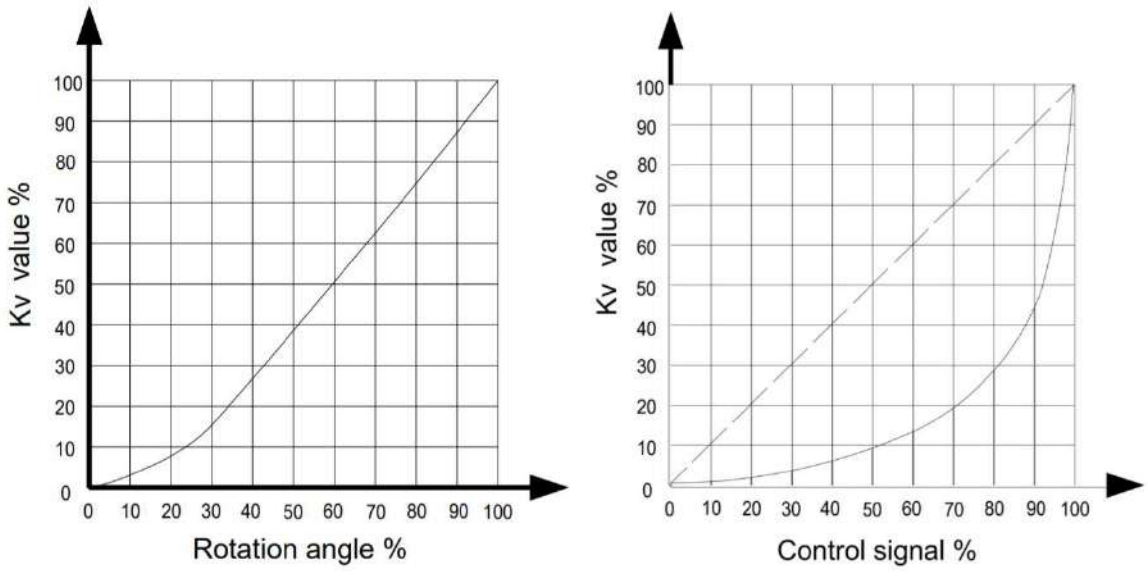

***Figure 3**: Natural characteristic (left) and Equal-percentage characteristic curves (right, solid line)*

$$K_v\% = \frac{K_v}{K_{v_s}} = \frac{1}{K_{v_s}} \frac{\dot{m_{ORC}}}{\rho_{in}} \sqrt{\frac{SG_{in}}{\Delta P}} \tag{1.1}$$

Table 3 contains the valve's main technical information:

Description	Value
Valve type	73.7 R
Nominal size [mm]	DN 80
Overall length	280 mm
Kv value at maximum flow (Kvs)	150 $m^3/h.bar^{0.5}$
Seat diameter	60 mm
Design pressure	63 bar
Drive data	
Positioner type	3730-4
Drive type	Pneumatic, R 200
Security position	Spring closes

***Table 3**: Throttling valve technical data*

1.2.2 Control System

A control system aims to provide automatic adjustment to a measured process variable to equal the value of a desired setpoint. The installed control system in MoNiKa is Siemens T3000, which is designed for the operation of high capacity power plants [13]. It provides all temperature, pressure, mass flow and positioning data, which are necessary for the modeling and optimization of the control loops. The software provides, additionally, a software PID controller.

A control loop contains all the elements that are required to adjust the controlled variable (Figure 4):

- a transmitter, which measures the controlled variable and whose signal is sent to the controller, where it is compared with the setpoint input;
- a controller, which calculates the error between the setpoint input and the measured process value, and, accordingly, sends an instruction to the actuator;
- an actuator, or final control element, which receives the controller output and adjusts the process in order to keep the controlled variable at (or as near as possible) the setpoint value;

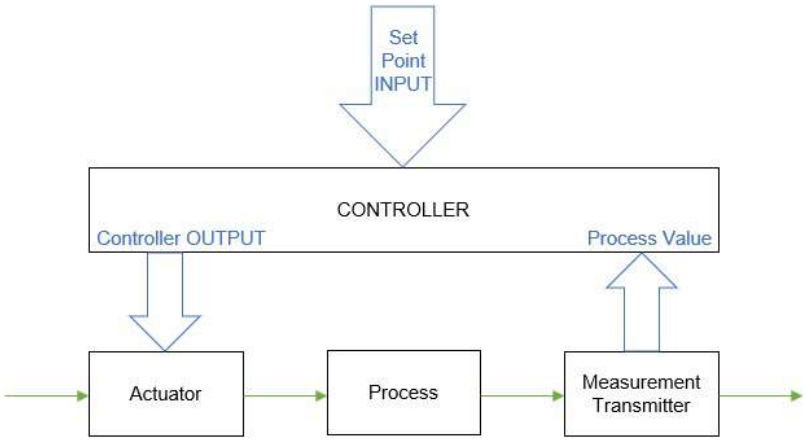

***Figure 4**: Block diagram of a simplified control loop*

It is possible to distinguish three types of variables in any given control loop. Firstly, the controlled variable is the process measured value whose control is wanted. The setpoint is the desired value of this variable. Secondly, the manipulated variable, which the actuator adjusts in order to maintain the controlled variable at its desired value. And finally, the disturbances are all the process variables that, may or may not be measured, affect the controlled variable, and cannot be directly manipulated in the same loop.

Three control loops are studied and optimized in this work, each concerning one of the power plant's main component described previously: the propane mass flow is controlled in the main pump loop. The setpoint is entered in the controller, whose output signal provides the frequency converter attached to the pump's electric motor the required rotational speed to reach the desired mass flow value. As it was discussed previously, only the pump speed and inlet density are needed to define the operational point in this kind of pump. However, taking into account that the inlet flow is ~0.05 MPa above saturation point, density changes can be considered negligible in the pump inlet. Lastly, mass flow control does not affect the pump's discharge pressure, which is controlled by the throttling valve loop.

The support pump loop controls its pressure difference. 0.05 MPa of pressure head are needed, at least, in order to avoid cavitation in the main pump. Similarly to the previous case, a frequency converter receives the controller output and provides the motor the rotational speed needed to meet the pressure difference setpoint. Because the mass flow is already controlled in a separate loop, only pump speed is required to define the centrifugal pump operation point. Inlet density can be negligible for the same reasons.

The actual configuration on MoNiKa follows a fixed live steam pressure control strategy, in which the pressure at which heat is supplied to the working fluid must remain constant. This control happens in the throttling valve. While the discharge pressure is defined by the condenser, the inlet is controlled in a third control loop. The valve positioner, working as the actuator, receives the controller signal and adjusts the rotational angle to provide the pressure difference that is required to maintain the inlet pressure at the desired value. Since they affect the controlled variable, mass flow and inlet density are disturbances for this process.

A summary of the variables involved in each control loop is presented in Table 4:

Main Pump	
Controlled Variable	Propane mass flow
Manipulated Variable	Pump Speed
Disturbance	-
Actuator	Frequency Converter
Transmitter	Mass flow sensor

Support Pump	
Controlled Variable	Pump pressure difference
Manipulated Variable	Pump Speed
Disturbance	Propane mass flow
Actuator	Frequency Converter
Transmitter	Pressure sensors (outlet – inlet)

Throttling Valve	
Controlled Variable	Live steam (inlet) pressure
Manipulated Variable	Valve's rotation angle fraction
Disturbances	ORC mass flow, inlet density
Actuator	Valve Positioner
Transmitter	Inlet pressure sensor

***Table 4**: Summary of control loops' variables and elements*

2 Dynamic Modeling and Simulation

This chapter presents the physical modeling procedure of the main components involved in each control loop. Discussion is made on how Simscape [9], the software tool used for this purpose, works and what inputs are needed. Then, simulation results are validated with the measured data. Finally, since a transfer function for each process is required to work on control design, calculations and results are presented.

2.1 Simscape Modeling

Considering that it is part of the MATLAB and Simulink environment [11], Simscape was chosen as the programming tool for the components modeling. It is a graphical tool that allows to create physical systems by assembling different components from its library into a schematic. These components include electrical, mechanical, digital, and fluid systems that can be integrated to conceive a model of a real process. The fact that control design of the final Simscape model can be performed in Simulink is a major advantage for this work.

The final goal is to obtain a model of both pumps, main and support, as well as the throttling valve, which could be able to reproduce, as near as possible, the dynamic response of the real components within the boundary conditions of the test runs that were previously carried out. Consequently, having available all the input data, the response of each model should closely match the measured data.

All fluid properties involved in this process were taken from REFPROP, which is the National Institute of Standards and Technology reference database [10]. A list of the properties required by Simscape to run the simulation is presented in Table 5.

Each element is firstly modeled individually, isolated from the rest components. In a final step, the three models are integrated in one single physical system.

Most of the modeling was done using blocks from the program's Thermal Liquid Library, which includes all the elements required for simulating fluid systems: pumps, valves, actuators, sensors, among others. The Mechanical Library was used for driveline purposes. Blocks chosen for each component are listed in Table 5, together with all technical properties and flow data inputs that are needed to fully characterize their correct operation. Technical information was taken from the manufacturer's datasheets, which were presented in the previous chapter.

Impressions of the models' arrangements in Simscape's graphical interface are available in the Appendix Section.

Fluid Properties	
Working temperature and pressure ranges	
Atmospheric pressure	
As temperature and pressure functions:	Density
	Thermal conductivity
	Kinematic viscosity
	Specific internal energy

Main Pump	
Block	Fixed-Displacement Pump
Block inputs	Displacement value
	Rotational speed and pressure gain ranges
	Volumetric and mechanical efficiency tables
Data inputs	Pressure (inlet and outlet)
	Inlet Temperature
	Rotational speed

Support Pump	
Block	Centrifugal Pump
Block inputs	Reference density
	Rotational speed and volumetric flow ranges
	Pressure head and brake power tables
Data inputs	Inlet pressure and temperature
	Mass flow
	Rotational speed

Throttling Valve	
Block	Flow Coefficient Parametrized Valve
Block inputs	Kv value at maximum flow
	Opening characteristics (equal-percentage)
	Rangeability
	Overall length
Data inputs	Temperature (inlet and outlet)
	Outlet pressure
	Mass flow
	Control signal fraction

***Table 5**: Simscape modeling inputs*

2.1.1 Results and Validation

Two sets of measurements were available to use as data inputs: on the one hand, the test run carried out during the 2019 Winter Semester for Luciano Gardella's Master Thesis Work [5], from now on referred to as data set #1. This hot run was done manually and is presented with a 10 second resolution. Setpoint data is, in this case, nonexistent.

On the other hand, the test run carried out by the ITES during the 2020 Summer Semester on 02.07.2020, will be referred to as data set #2 from now on. The control system was already active by the time this test was done, thus all setpoint data is available. Measurements are presented with a 1 second resolution. Because of these reasons, a decision was made to perform simulations using data set #2, while #1 was used for validation purposes.

A lapse of 3.5 hours (12600 seconds), out of more than 4.5 hours of duration for the whole Summer Semester test run, was used as simulation stop time. Startup and shutdown time intervals were not considered. All input data specified on Table 5 was available in an Excel sheet and was exported to the corresponding Simscape files.

Figure 5-A contains the comparison between the main pump's model response (orange line) and the real mass flow taken from data set #2 (grey line). Support pump's pressure difference responses are presented in Figure 5-B, and finally, comparison of the throttling valve's inlet pressure responses is shown on Figure 5-C.

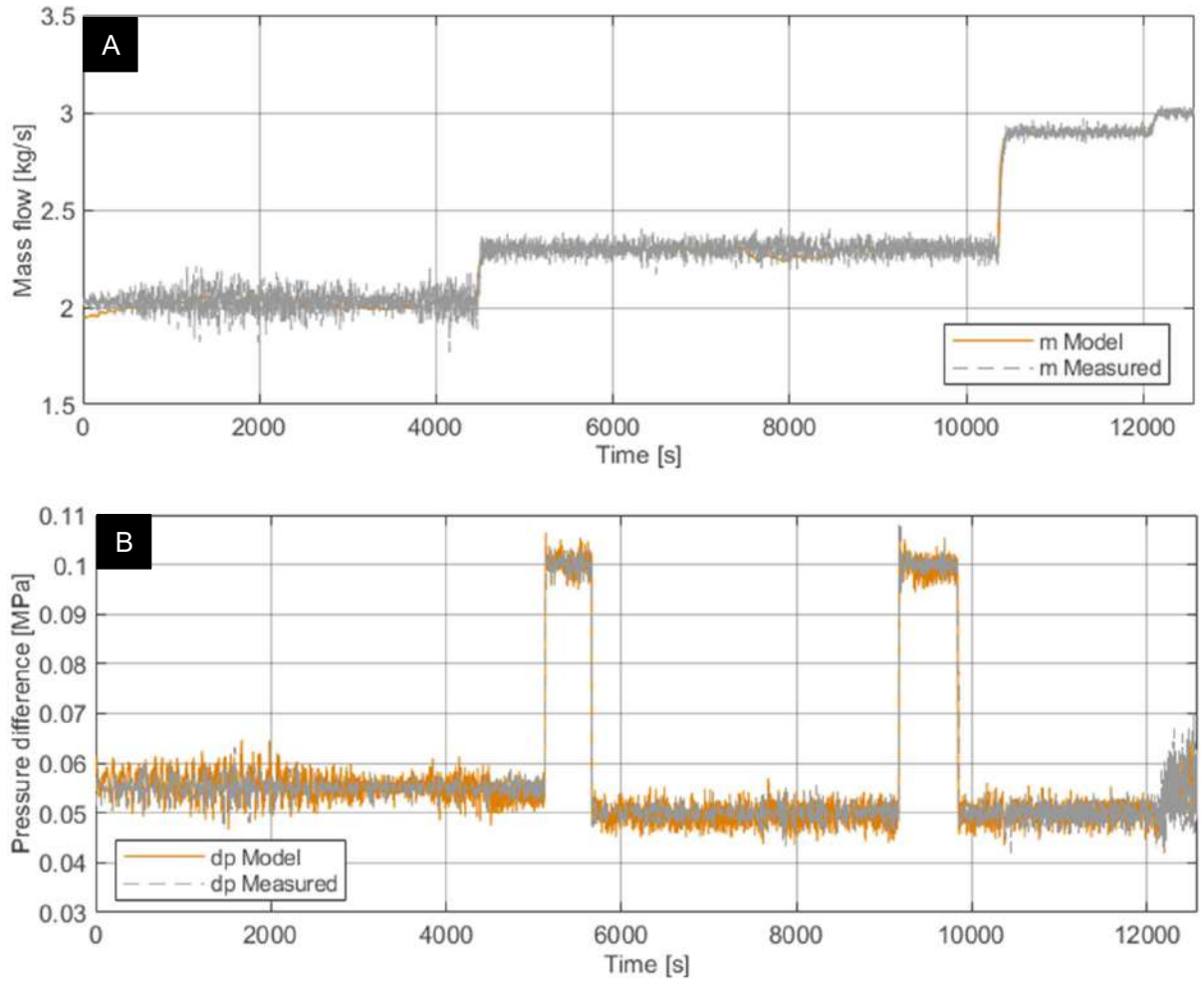

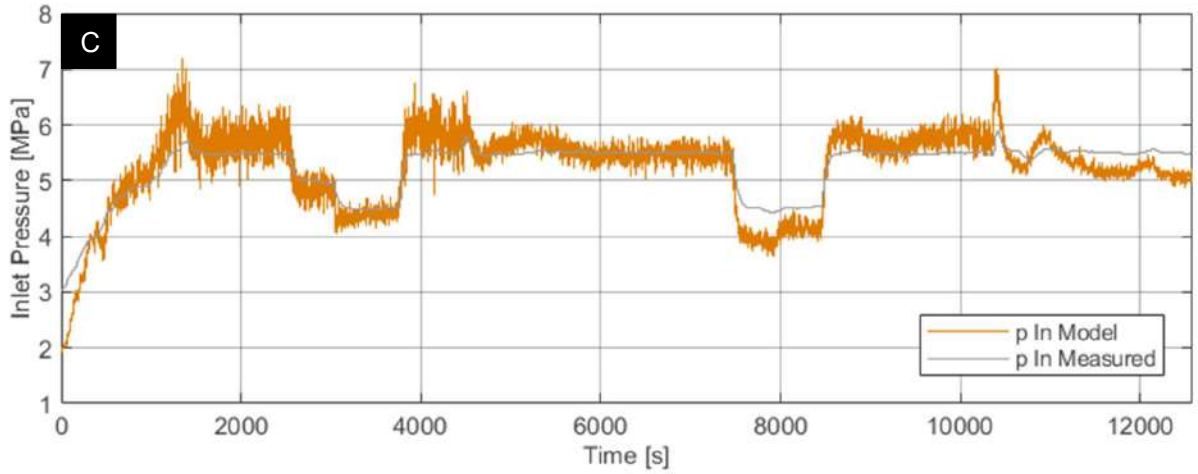

***Figure 5**: Comparison of responses of the three Simscape models with the measured data (set #2)*

All three models provide a satisfactory fit to the experimental data. Without considering the level of noise present in the measured data, the shape of the model response is, in all cases, similar to the data along the entire time lapse, and the response times match as well. The slight differences that can be seen in Figure 5-C could be explained by the numerical conversion between the real input data the model uses (control signal fraction), and the available measured data (rotational angle fraction). This conversion is made following the curves shown on Figure 3.

In order to validate these results, simulations are performed once again, this time using set #1 as experimental data. The physical models remained untouched and the same time lapse as the previous case was used. Validation results are presented in Figure 6 in the same order.

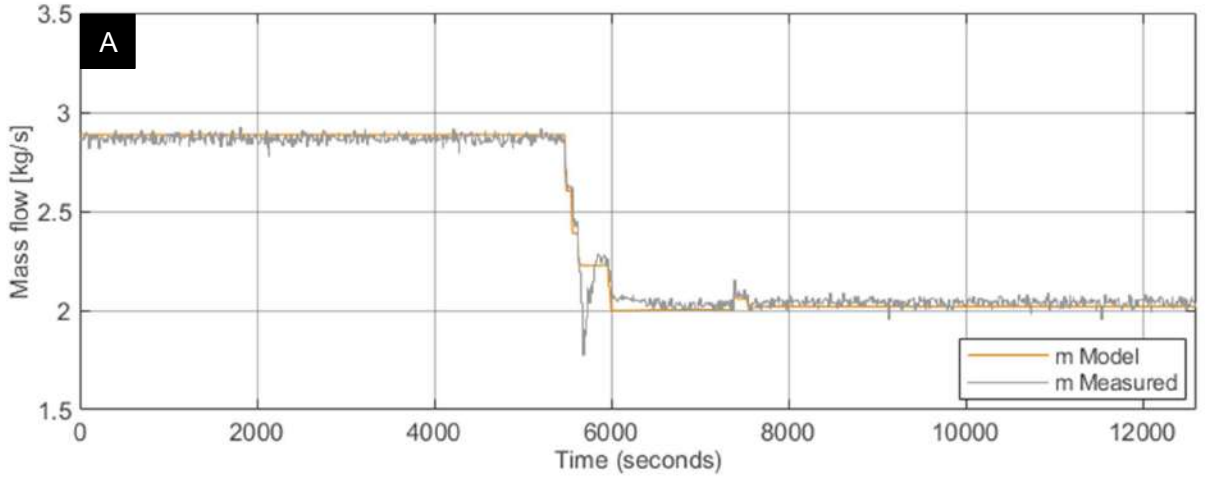

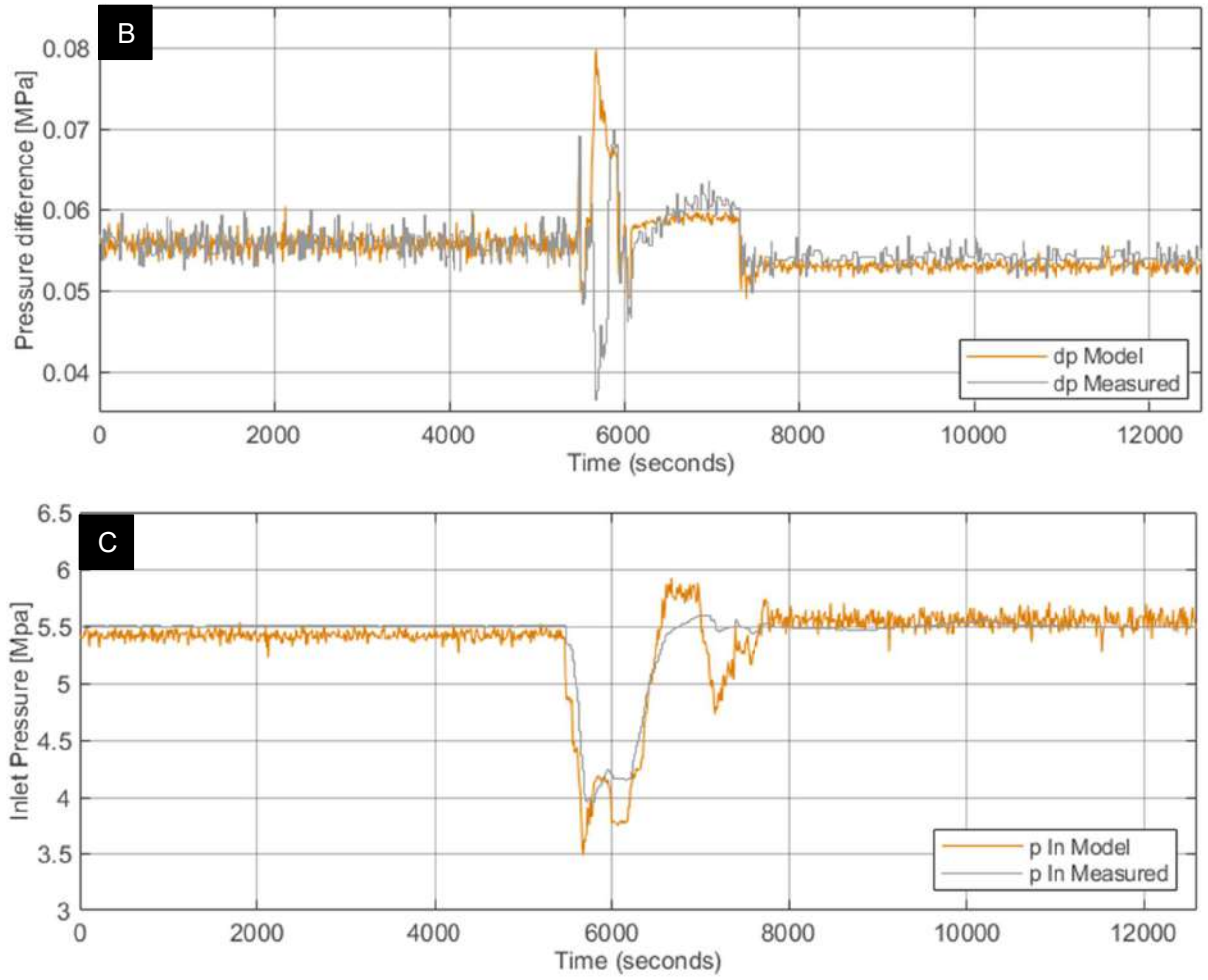

***Figure 6**: Comparison of responses of the three Simscape models with the measured data (set #1)*

All three models give, again, an adequate fit to the experimental data, except for the brief time lapse at which sudden changes in mass flow occur (between time ~5700 and ~6000 seconds). Each model, however, recover stability at the same rate as the corresponding real component.

As the components' models have been validated within the boundary conditions at which both sets of experimental data were taken, they become a useful and reliable tool for control design. Nevertheless, before optimizing the control system, a transfer function for each process must be obtained.

2.2 Process transfer functions

Having in mind the goal of this thesis work, it is convenient to obtain transfer functions that could simplify the analysis and optimization of the control system. A transfer function is an s-domain algebraic expression that relates the dynamic behavior of the input and outputs of a given process model in a compact way.

If a linear differential equation for that process is available, a transfer function can be derived from it applying Laplace transformation. However, in the case of the three power plant components studied in this work, such type of equations cannot be obtained. Hence, the following MATLAB command is used to derive them using the measured data as inputs and outputs [11]:

$$sys = tfest(data, np, nz)$$

The command *tfest* estimates the s-domain transfer function for each process. The parameter *data* contains the time-domain estimation data, which is exported to MATLAB from the same Excel sheets used for modeling, while the parameters *np* and *nz* represent the number of poles and zeros of the estimated transfer functions.

As it was previously mentioned, data set #1 does not contain setpoint data. Thus, considering this information is necessary for control system design and analysis, the process functions were estimated from data provided solely by set #2.

On the one hand, in the case of the main pump, the process input is the rotational speed, while the output is the mass flow. As a consequence, a single input-single output transfer function is estimated. On the other hand, the rest of the components' operation cannot be defined by a single input: the support pump requires mass flow and rotational speed, and the throttling valve needs mass flow, rotation angle fraction and inlet density. These are cases of multiple input-single output transfer functions, and because of the additive property inherent to these functions, the final output value is calculated adding every individual input contribution.

2.2.1 Results and Discussion

Different combinations of pole and zeros numbers were evaluated, and judging by the results, it was decided in all three cases to estimate second order transfer functions with one zero. MATLAB's programming code is shown in the Appendix Section. Using the same time lapse as the previous case, function estimations are shown on Table 6:

Main Pump	
Input	Rotational speed - rpm
Ouput	Mass flow - m
Transfer function	$\frac{m}{rpm} = \frac{0.133s + 0.0004164}{s^2 + 63.87s + 0.2037}$
Support Pump	
Inputs	Rotational speed - rpm Mass flow - m
Ouput	Pressure difference - dp
Transfer function	$dp = \frac{0.000134s + 3.19x10^{-8}}{s^2 + 1.252s + 0.000581} rpm + \frac{-0.0127s - 1.58x10^{-6}}{s^2 + 0.23s + 8.69x10^{-5}} m$

Throttling Valve	
Inputs	Rotation angle fraction - RAF
	Mass flow - m
	Inlet density – ρ (*)
Ouput	Inlet pressure - p In
Transfer function	$p\ In = \frac{-0.1587 - 6.243x10^{-8}}{s^2 + 0.0122s + 7.5x10^{-9}}\ RAF + \frac{-0.0315s + 5.913x10^{-6}}{s^2 + 0.0168s + 2.05x10^{-5}} m + \frac{0.00042s + 3.59x10^{-9}}{s^2 + 0.02s + 2.36x10^{-7}} \rho$

(*) Calculated at a constant inlet pressure of 5.5 MPa

***Table 6**: Transfer functions, inputs, and output variables*

Comparison of the functions' outputs with the measured data is presented on Figure 7, following the same order and structure as the modeling results:

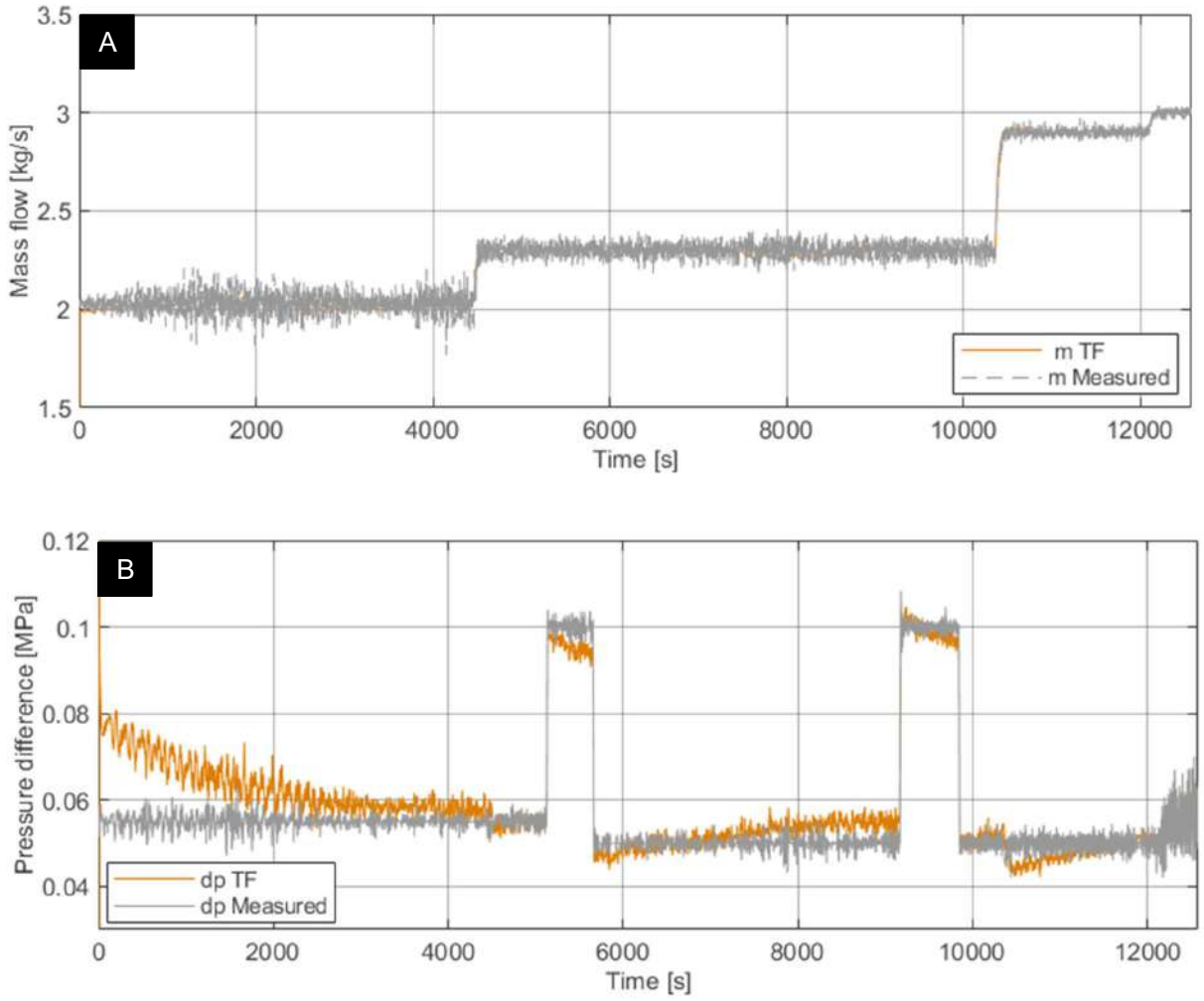

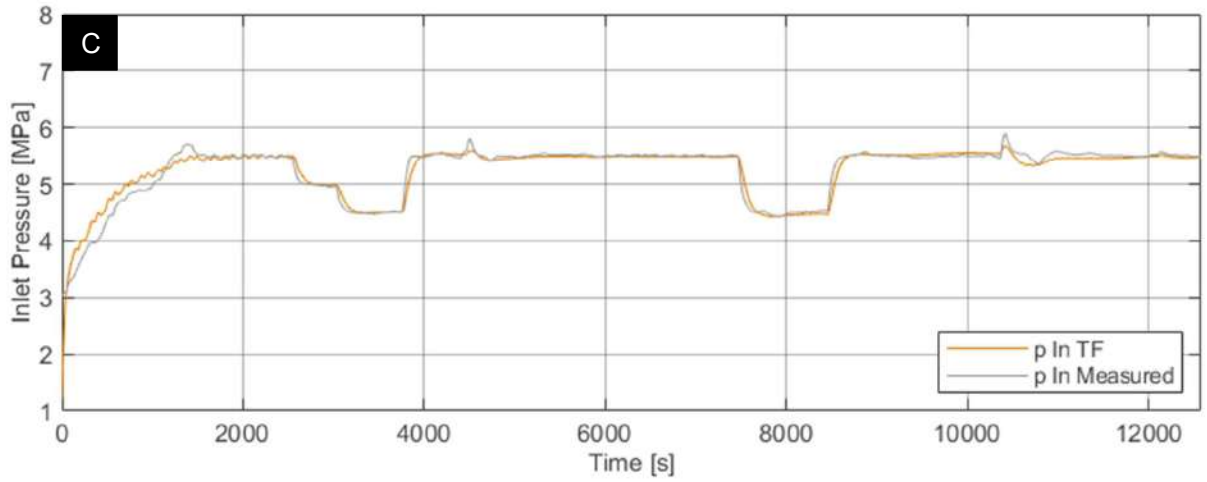

***Figure 7**: Comparison of the three transfer function outputs with the corresponding measured data (set #2)*

As it can be seen in Figures 6-A and C, transfer functions outputs thoroughly follow the speed and qualitive features of the systems' measured responses, providing an optimal fit to data. This does not happen all along Figure 7-B. In this case, the shape of the function response is crooked in comparison with the experimental data. This distortion, however, appears around the real values of steady-state gain. Thus, considering the main purpose of these functions is to simplify the controllers' parameters calculation, with the controllers and physical models being part of a closed-loop system, the level of fit to data these functions present is satisfactory.

3 Control Design

The aim of this chapter is to present the theory needed to optimize the power plant's control system. Feedback control basics are introduced, together with its block diagram representation and PID controllers operating principles. A detailed description of MoNiKa's control system is then given, with the focus put on the controller's transfer function. Finally, tuning methods are presented, as well as the stability and sensitivity design criteria.

3.1 Background Theory

Following the introductive control theory presented on section 1.2.2, it is critical to acknowledge one distinctive aspect of the system illustrated in Figure 4: as the process output value is continuously being measured in-line, its signal is sent back as an input to the controller, which compares it to the setpoint and, consequently, sends the actuator the appropriate corrective action required to keep the controlled variable at its desired value. Systems presenting this dynamic behavior, characterized by the process output being routed back to the system as an input, are known as feedback control loops or closed-loop systems.

Block diagrams and transfer functions provide useful information about a closed-loop system. A standard version of a feedback control loop diagram is shown in Figure 8. While blocks contain a transfer function for each element that conform the system, arrows indicate the flow direction of all signals. Notation is based on Seborg et al. [12], and it is indicated on Table 7:

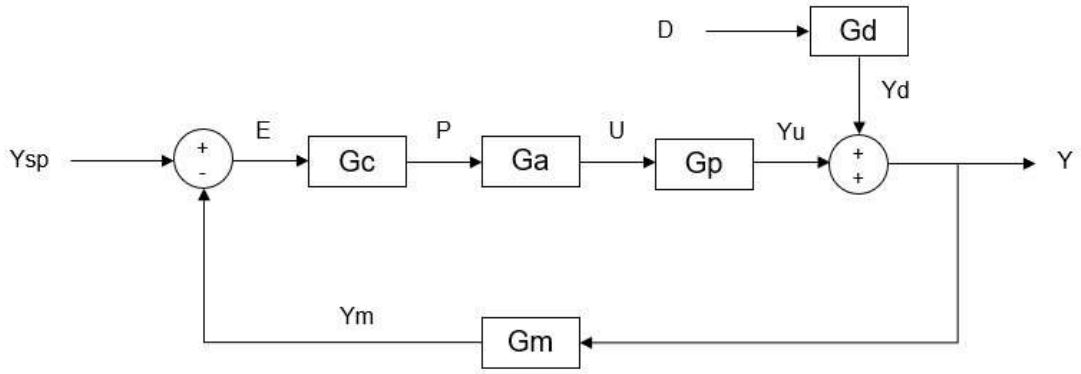

Figure 8: *Standard feedback control loop block diagram*

Signals		**Blocks**	
Ysp	Setpoint	Gc	Controller transfer function
E	Error	Ga	Actuator transfer function
P	Controller Output	Gp	Process transfer function
U	Manipulated Variable	Gd	Disturbance transfer function
Yu	Change in Y due to U	Gm	Transmitter transfer function

D	Disturbance Variable
Yd	Change in Y due to D
Y	Controlled Variable
Ym	Measured value of Y

Table 7: *Standard closed-loop system notation*

With the help of block diagram algebra, two useful expressions can be derived from Figure 8. To begin with, the open-loop transfer function, which is obtained assuming that the feedback loop is opened, and which relates Ym to Ysp:

$$G_{OL} = G_c G_a G_p G_m \tag{3.1}$$

Secondly, the closed-loop transfer function for setpoint and disturbance changes:

$$Y = \frac{G_c G_a G_p G_m}{1 + G_{OL}} Y_{sp} + \frac{G_d}{1 + G_{OL}} D \tag{3.2}$$

These expressions, together with all elements' transfer functions, provide the information required to analyze the stability, sensitivity, and performance of a closed-loop system. An ideal feedback control system should provide the process the proper dynamic and steady-state response characteristics. As Seborg et al. indicate in their textbook [12], control design should pursue the following performance criteria:

- *"The closed-loop system must be stable.*
- *The effects of disturbances are minimized, providing disturbance rejection.*
- *Rapid, smooth responses to set-point changes are obtained, that is, good set-point tracking.*
- *Steady-state error (offset) is eliminated.*
- *Excessive control action is avoided.*
- *The control system is robust, that is, insensitive to changes in process conditions and to inaccuracies in the process model."*

In order to achieve these requirements, it is necessary to optimize the controllers' performance. There are three PID controllers installed in MoNiKa, one for each of the control loops involved in this work. Proportional-integral-derivative (PID) controllers are the most widely used among feedback loops. They calculate an error as the difference between the setpoint and measured process value, and, as their name indicates, apply corrective action based on the proportional, integral, and derivative terms.

The parallel form of a PID controller with derivative filter, which is the type of controller configuration used in MoNiKa, is given by the following transfer function:

$$G_c = P\left(1 + \frac{I}{s} + \frac{D}{\frac{1}{N} + \frac{1}{s}}\right) \tag{3.3}$$

Where P, I, and D stand as the proportional, integral, and derivative gains; N being the derivative coefficient or filter. These values conform the controllers' parameters.

Equation 3.3 shows that this type of controllers can be seen as three separate blocks operating in parallel, each one of them contributing with one type of control action:

- Proportional control alone produces an output that is proportional to the error signal, and steady-state error, or offset, is inevitable.
- Integral control provides offset elimination and accelerates the response towards the desired value. Because the output depends on the integral of the error signal, little control action is taken until some error is accumulated.
- Derivative control anticipates the error behavior by following its rate of change, thus stabilizing the response, and decreasing its settling time. A derivative filter is required to prevent amplification of noise due to random process measurement fluctuations. Moreover, because it is more sensitive to higher frequency inputs, derivative action is often discarded in processes with noisy measurements.

Having in consideration that the processes' models are available and have been validated, control system optimization is achieved by finding a set of controllers' parameters that are able to fulfill the performance criteria mentioned earlier. The process of adjusting these values is known as control tuning.

3.2 MoNiKa's Control System

As it was mentioned on Section 1.2.2, MoNiKa's control system is Siemens T3000 [13]. The PID controllers are integrated with the software, and its algorithms are implemented with digital signal pathways -or networks-, used for data transmission.

Continuous-time transfer functions were considered until now. However, digital controllers' inputs and outputs are sampled (digital) signals, rather than continuous functions of time (analog). Integral and derivative terms of Equation 3.3 must be therefore replaced by a finite difference approximation in order to obtain a discrete-time version of the parallel form of PID controller with derivative filter.

In order to replicate the Simulink tuning results in the Siemens T3000 control system, the compensators formulas used by each program must have a similar form. Considering that MoNiKa's control system provides the following controller formula [14]:

$$G_c = GAIN\left(1 + \frac{t_s}{TN} + \frac{TD}{T1 + \frac{t_s}{2}}\right) \tag{3.4}$$

the Forward Euler, or left-hand rectangular approximation, is used in Simulink for the integral term, while the Trapezoidal or bilinear approximation is selected for computing the derivative filter method. Consequently, all Simulink simulations are performed using this resulting expression:

$$G_c = P\left(1 + I\frac{t_s}{z-1} + \frac{D}{\frac{1}{N} + \frac{t_s}{2}\frac{z+1}{z-1}}\right) \tag{3.5}$$

Where ts represents the sampling time, which is the period between successive controlled variable measurements, and z is the discrete time parametrization symbol.

Although equations 3.4 and 3.5 may look different, by using the conversions presented in Table 8, it is possible to see they have the same form:

Parameter	MoNiKa Form	Simulink Form	Conversion
Proportional Gain	GAIN	P	P = GAIN
Integral Gain	TN [s]	I	I = 1/TN
Derivative Gain	TD [s]	D	D = TD
Filter coefficient	T1 [s]	N	N = 1/T1

Table 8: *Controllers' formulas conversions*

From now on, Simulink's notation is used in this work. However, it is still crucial to use these conversions in order to implement the final tuning results in the real control system. The controllers' parameters used during the Summer Semester hot run, form which data set #2 was obtained, are shown on Table 9:

Control Loop	P	I	D	N
Main Pump	1.00	1.00	0.00	-
Support Pump	3.00	2.00	0.00	-
Throttling Valve	0.02	0.25	1.00	0.33

Table 9: *PID controllers' parameters used during 02.07.2020 hot run*

Siemens T3000 control system also provides the possibility to program the setpoint data. During the mentioned test run, setpoint values for all three control loops were entered as ramps, each with a specified slope:

- Main pump loop: ± 0.2 kg/s/s
- Support pump loop: ± 0.125 bara/s
- Throttling valve loop: ± 2 bar/s

With the purpose of obtaining the actuator gains (Ga), the system's internal program calculations for each controller are studied. These gains provide the relation between each controller output (software's digital signal) and the corresponding process input:

- Main pump loop: Ga = 14.7 rpm / rotational speed %
- Support pump loop: Ga = 45 rpm / rotational speed %
- Throttling valve loop: Ga = 0.01 control signal fraction / control signal %

Finally, regarding the transmitter's transfer functions (Gm), a signal transport delay of 1 second was implemented as a design conservatism criterion in all three control loops:

$$G_m = e^{-s} \tag{3.6}$$

3.3 PID Controller Tuning

In order to achieve satisfactory control, the preliminary controller parameters shown on Table 9 need to be adjusted. The tuning methods chosen for this purpose are selected based on the configuration and characteristics of the control loops.

3.3.1 Main and Support Pump

Both main and support pump loops follow the standard feedback configuration presented on Figure 8. Moreover, during the Summer Semester test run, proportional-integral controllers were used in both cases. The reason of this choice was the intention to pursue a conservative controller design. Thus, as a first guess, a practical approach was followed to only use the proportional and integral terms. Also, the level of noise in the mass flow measurement made it reasonable to discard the derivative action.

Considering these similarities, both sets of PI controllers' parameters are tuned following the Continuous Cycling Method, which is prominent in process control literature and widely used in the industry. Published by Ziegler and Nichols in 1942 [15], it is based on an on-line trial-and-error procedure whose purpose is to determine the ultimate gain and period of the closed-loop response, which are required to calculate the PID settings using a series of tuning relations.

The ultimate gain (Kcu) and period (Pu) refer to the numerical value of both the constant amplitude and period of the sustained, continuous oscillation produced in the closed-loop response once the process is pushed to its marginal stability limit. These values can be obtained empirically eliminating the controller's integral and derivative action and manually introducing small setpoint changes while increasing the proportional gain. Consequently, Kcu can be defined as the largest value of P that

results in a stable closed-loop system. However, this procedure can be time-consuming and produce unstable operation. Alternatively, they can be determined from a frequency response analysis.

Frequency response characteristics of a given transfer function can be conveniently read on a Bode plot. Each diagram consists of two plots, in which the transfer function's amplitude ratio and phase angle are plotted as a function of frequency.

Since all transfer functions involved in both control loops have been determined, it is possible to calculate the open-loop transfer functions (3.1) on MATLAB. Then, in order to obtain Kcu and Pu, MATLAB's 'margin' command is used on the open-loop transfer function, while considering a proportional-only controller with a unitary gain. This command plots the Bode response and indicates the ultimate gain, as well as the critical frequency (ωc) which is the frequency at which the function's phase angle equals -180°, in rad/s. Pu can be obtained as 2π/ωc.

Finally, two sets of controllers' settings are calculated using the Ziegler-Nichols (ZN), and the Tyreus-Luyben (TL) controller tuning relations, which provide more conservative results [16]. Both sets of relations are showed on Table 10:

ZN	P	I	D
PI	0.45Kcu	1.2/Pu	-
PID	0.6Kcu	2/Pu	Pu/8
TL	P	I	D
PI	0.31Kcu	0.454/Pu	-
PID	0.45Kcu	0.454/Pu	Pu/6.3

Table 10: *Ziegler-Nichols and Tyreus-Luyben PI and PID controller tuning relations*

Selection of the final settings is made based on the performance and the stability and sensitivity values.

3.3.2 Throttling Valve

Analyzing the control system's internal programming, two distinctive characteristics can be appreciated in the throttling valve's control loop, which make its behavior, and thus its treatment, different from the previous two:

- A feedforward constant equal to one is added to the controller's output.
- The error signal is calculated as the measured variable of Y minus the setpoint, (E = Ym-Ysp), this being the exact opposite of the standard configuration.

The resulting block diagram is shown on Figure 9:

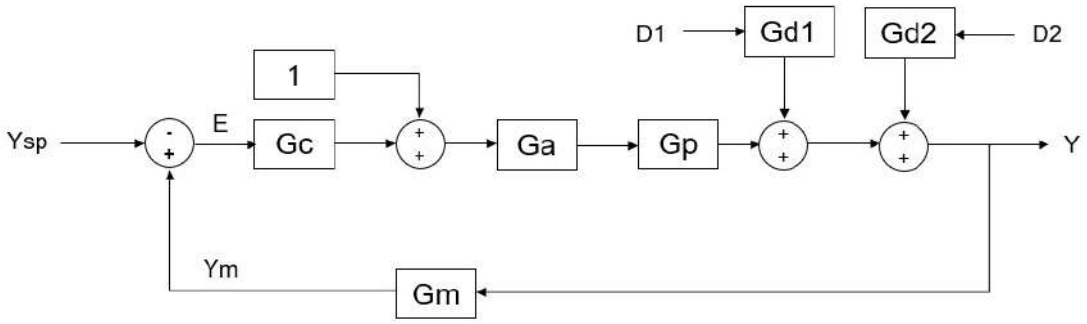

Figure 9: *Throttling valve's control loop block diagram*

Both open and closed-loop transfer functions are naturally modified by these two singularities. In order to be able to operate in MATLAB and proceed with the tuning design, these expressions are re-arranged using block diagram algebra:

$$G_{OL} = G_a G_p G_m \left(\frac{1}{Y_{sp}} - G_c \right) \tag{3.7}$$

$$Y = \frac{-G_c G_a G_p G_m}{1 - G_c G_a G_p G_m} Y_{sp} + \frac{G_{d_1}}{1 - G_c G_a G_p G_m} D_1 + \frac{G_{d_2}}{1 - G_c G_a G_p G_m} D_2 + \frac{G_a G_p}{1 - G_c G_a G_p G_m} \tag{3.8}$$

Since all the control loop components' transfer functions have already been determined, the Continuous Cycling Method can now be implemented as discussed previously. Based on the controller settings used during the Summer Semester test run, derivative action is not discarded in this case. Following Seborg's recommendation [12] for the filer coefficient calculation, this guideline is used:

$$N = \frac{1}{\alpha D}, 0.05 \leq \alpha \leq 0.2 \tag{3.9}$$

3.4 Stability and Sensitivity Analysis

Two of the main characteristics the control design should pursue are: the stability of the closed-loop system operating while different process perturbations occur, and its low sensitivity to setpoint and disturbance changes. All notation is taken form Seborg et al. [12].

Firstly, relative stability of a control loop can be measured by the gain margin (GM) and the phase margin (PM). Based on the Bode stability criterion, which indicates that a closed-loop system is stable if the amplitude ratio of the open-loop system at the gain crossover frequency (ARc) is smaller than one, these concepts can be determined as follows:

$$GM = \frac{1}{AR_c} \tag{3.10}$$

$$PM = 180° + \Phi_g \tag{3.11}$$

Where Φ_g denotes the phase angle of the open-loop system at the gain crossover frequency. Both values are presented on a Bode plot when the 'margin' command is entered on MATLAB.

An equivalent to the Bode stability criterion would be that the gain margin should always be greater than one. Consequently, this value provides a metric on how much the feedback controller gain can increase before the system becomes unstable: the closer the gain margin is to one, the closer to instability. Regarding the phase margin, this value, which is presented in degree units, indicates the amount of additional delay time that can be introduced on the feedback system before it reaches a continuous oscillatory response: the smaller the phase margin, the closer to instability. On the contrary, larger values of gain and phase margin correspond to slow, sluggish responses.

In his textbook [12], Seborg et al. indicate a general guideline for control design, which will be considered when selecting each set of controller settings:

"In general, a well-tuned controller should have a gain margin between 1.7 and 4.0 and a phase margin between 30° and 45°".

Secondly, sensitivity to setpoint and disturbance changes in a closed-loop system can also be measured, in this case by defining two sensitivity functions. Based on the standard closed-loop transfer function (3.2), and assuming for analysis purposes that Gd = 1, then the following expressions can be derived:

$$S = \frac{Y}{D} = \frac{1}{1 + G_c G_a G_p G_m} \tag{3.12}$$

$$T = \frac{Y}{Y_{sp}} = \frac{G_c G_a G_p G_m}{1 + G_c G_a G_p G_m} \tag{3.13}$$

S and T represent the sensitivity functions and indicate the closed-loop transfer functions for disturbances and setpoint changes, respectively.

In the case of the throttling valve, because the closed-loop transfer function differs from the standard version, so do the sensitivity functions:

$$S = \frac{1}{1 - G_c G_a G_p G_m} \tag{3.14}$$

$$T = \frac{-G_c G_a G_p G_m}{1 - G_c G_a G_p G_m} \tag{3.15}$$

The maximum values of the sensitivity functions' amplitude ratios, M_S and M_T respectively, provide useful metrics for sensitivity and robustness. Using MATLAB's command 'bodemag', it is possible to plot the magnitude frequency response of these functions. In other words, it enables to visualize the M_S and M_T values and their respective frequencies.

Since all three controllers contain integral actions, it is expected that no offset exists for setpoint or disturbance changes. Thus, at low frequencies the closed-loop system should not be sensitive to these changes: $S \rightarrow 0$, and $T \rightarrow 1$. Ideally, the control system should be designed to rapidly and smoothly reach the new steady state when a setpoint change occurs, and also to ensure that disturbances perturb as less as possible the system's response. These goals can be translated in the following way: it is desired to maintain T's amplitude ratio at unity and S's amplitude ratio minimized as high frequency as possible.

Because there is a tradeoff between performance and sensitivity, Seborg et al. [12] recommend the following guideline:

"For a satisfactory control system, M_T should be in the range of 1.0 - 1.5, and M_S should be in the range of 1.2 - 2.0".

Another concept used for comparing setpoint tracking performance, together with M_T, is the bandwidth (BW). It is defined as the frequency at which T's amplitude ratio equals 0.707. Because it is inversely proportional to the system's settling time, this value provides a useful metric to the speed of response. Thus, the larger the bandwidth, the faster the closed-loop system responds to setpoint changes.

MATLAB's programming codes are shown in the Appendix Section.

4 Results

Beginning with the calculation of controller settings, the stability and sensitivity results for each of the three sets of parameters are then presented. Followed by a comparison of setpoint and disturbance responses given by each set, a discussion on the results and performance is afterwards made. Finally, once the best set of controller settings has been selected, the response of each control loop is evaluated in the Simscape models.

4.1 Main Pump Loop

The ultimate gain and period corresponding to the main pump control loop were determined following the frequency response analysis previously described. Their values are: Kcu = 32.7, and Pu = 2 seg. In the first place, Table 11 shows the two sets of controller parameters calculated using the Ziegler-Nichols (ZN) and Tyreus-Luyben (TL) tuning relations, as well as those used during the Summer Semester test run (SSTR):

Set	P	I
SSTR	1.0	1.00
ZN	14.7	0.60
TL	10.1	0.23

Table 11: *Main pump's Summer Semester, Ziegler-Nichols and Tyreus-Luyben PI controller settings*

Secondly, MATLAB's Bode and sensitivity functions' magnitude plots are presented on Figure 10. Each pair of diagrams correspond to a set of controller parameters. Gain and phase margins can be read on the Bode plots, while M_T, M_S, and bandwidth values are shown on top of the sensitivity curves.

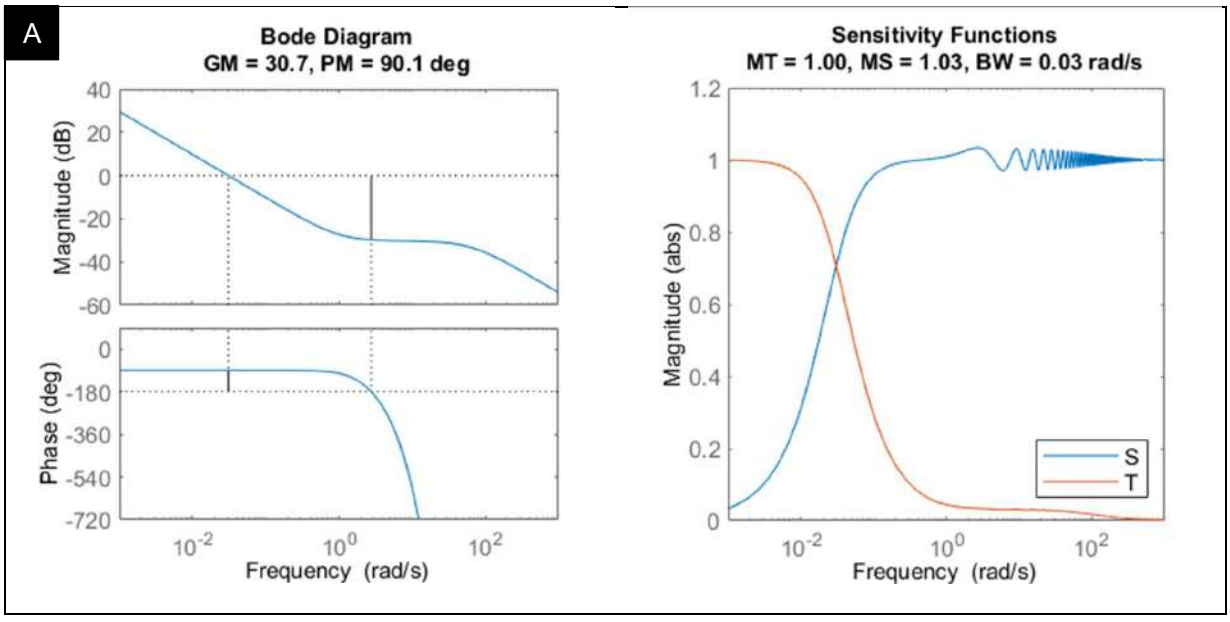

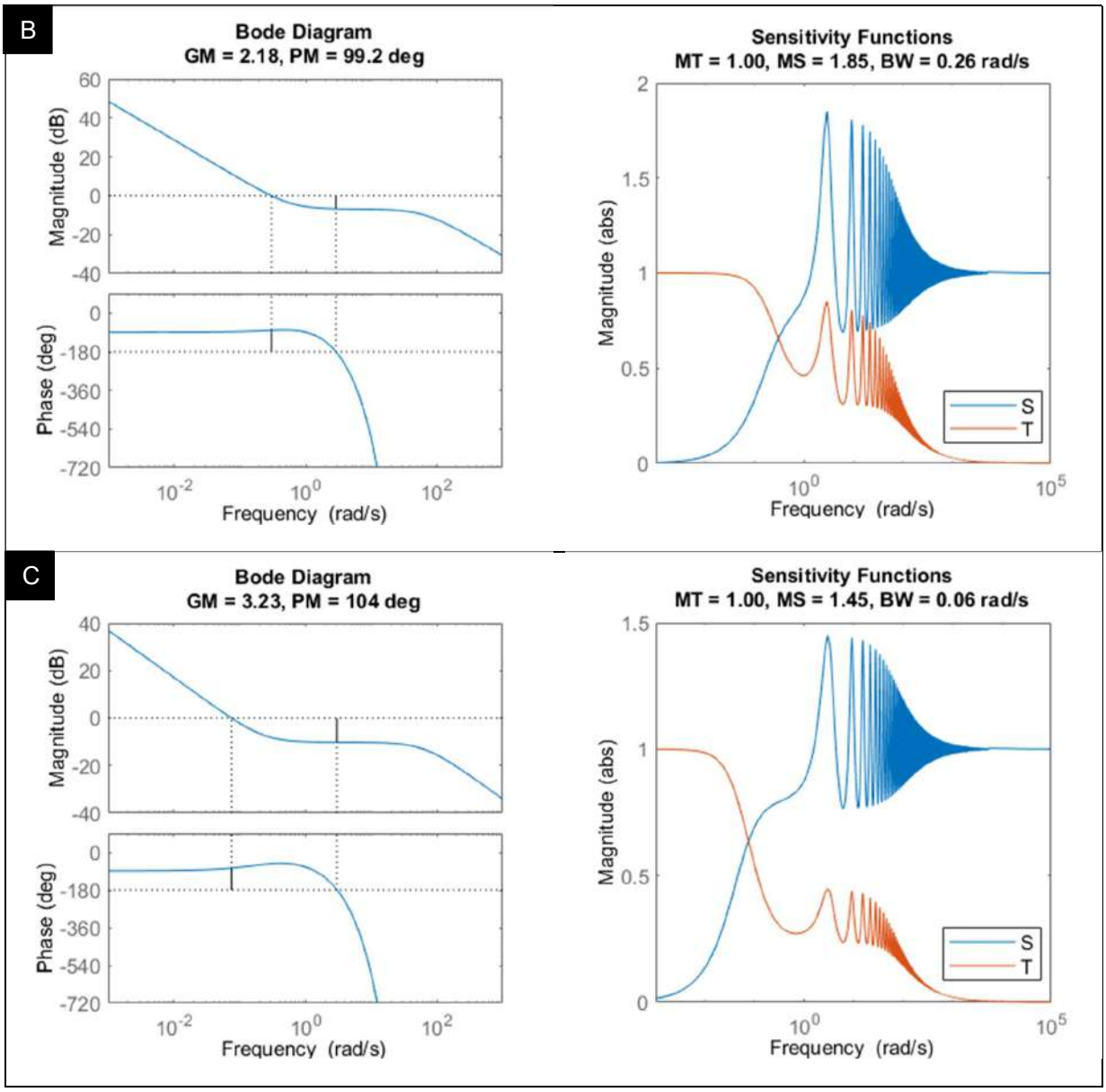

***Figure 10**: Main pump's Bode and sensitivity functions plots for the three sets of parameters. A) SSTR, B) ZN, C) TL.*

Lastly, a comparison of the closed-loop responses using each set of parameters is presented on Figure 11. Made on Simulink using the process transfer functions, this plot contains a unitary setpoint change at time 0. The discrete-time PI controllers are set with a sample time of 1 second.

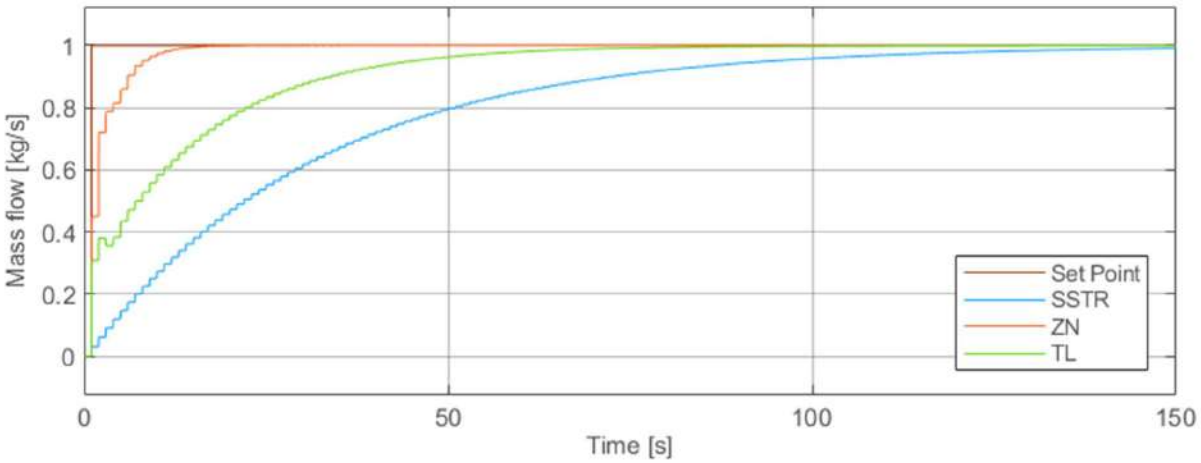

***Figure 11**: Main pump's closed-loop responses for the three set of parameters: SSTR, ZN, and TL. A unitary setpoint change occurs at time 0. Sample time = 1 sec.*

As Figure 11 shows, both sets of calculated parameters provide faster -but still smooth- responses than MoNiKa's default controller settings. The stability and sensitivity results in Figure 10 reinforces this idea: compared to the other two, SSTR's closed-loop gain margin, which is almost 8 times larger than the recommended value, indicates that its parameters are conservative and produce sluggish, slow responses. Moreover, bandwidth values show that ZN and TL's settings provide responses which are 8.6 and 2 times faster, respectively.

Phase margin values are in all three cases greater than what the design guideline specifies, which reveals that more additional delay time could be present in the closed-loop before reaching the instability limit. When comparing ZN and TL settings, both M_T and M_S, as well the gain margin values, follow Seborg's recommendations, which ensures that performance and robustness goals are achieved in both cases. The key difference remains in how much rapidly the closed-loop system responses when using ZN parameters: 4.3 times faster than when using TL's, and 8.6 than SSTR's.

As a result, Ziegler-Nichols controller settings provide the best response among the three sets evaluated, while following the control design specifications.

4.2 Support Pump Loop

The ultimate gain and period corresponding to the support pump control loop are: Kcu = 32, and Pu = 3 seg. Firstly, Table 12 shows the controller settings:

Set	P	I
SSTR	3.0	2.00
ZN	14.4	0.40
TL	10.0	0.15

***Table 12:** Support pump's Summer Semester, Ziegler-Nichols and Tyreus-Luyben PI controller settings*

MATLAB's Bode and sensitivity functions' magnitude plots are presented on Figure 12:

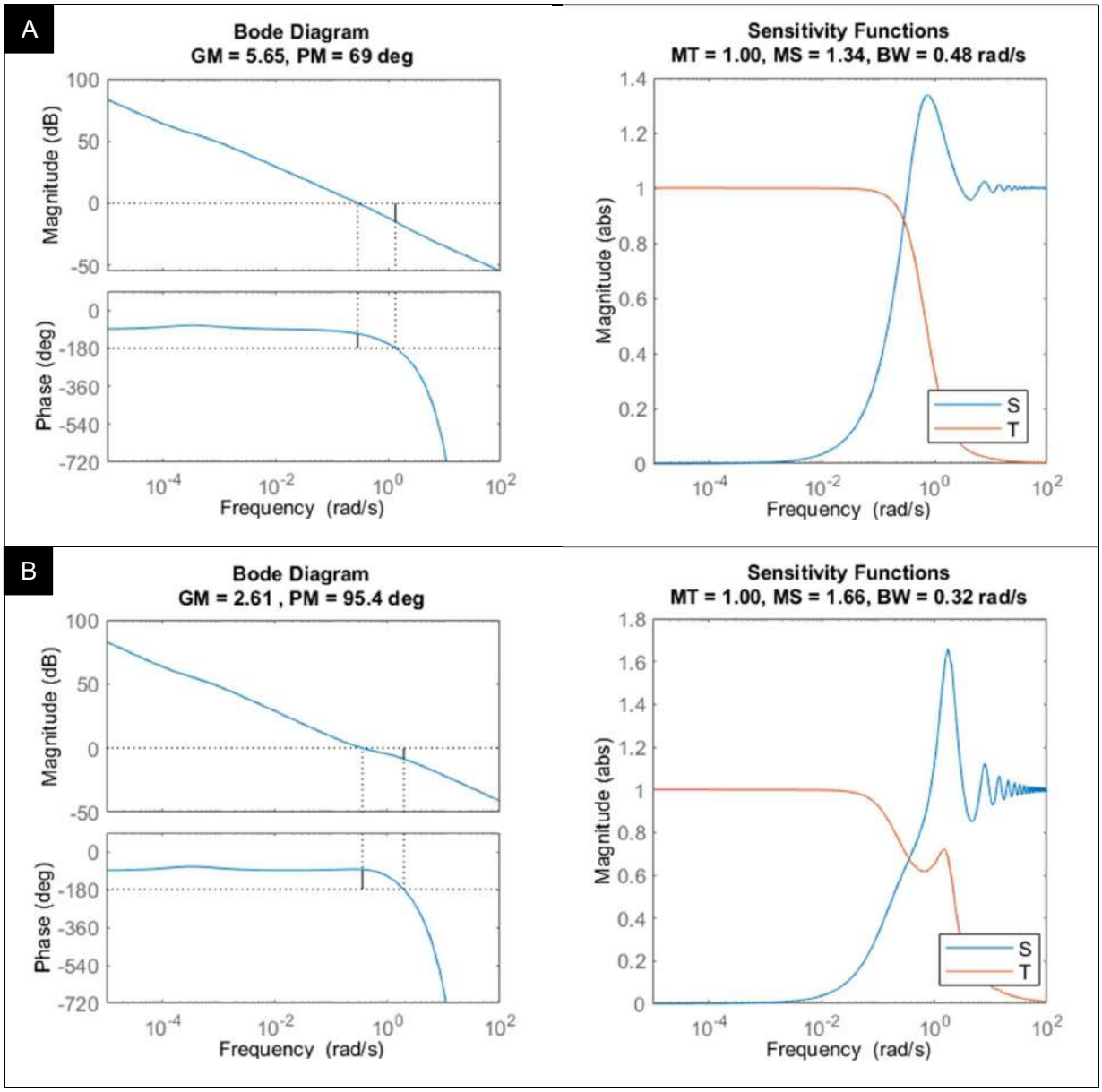

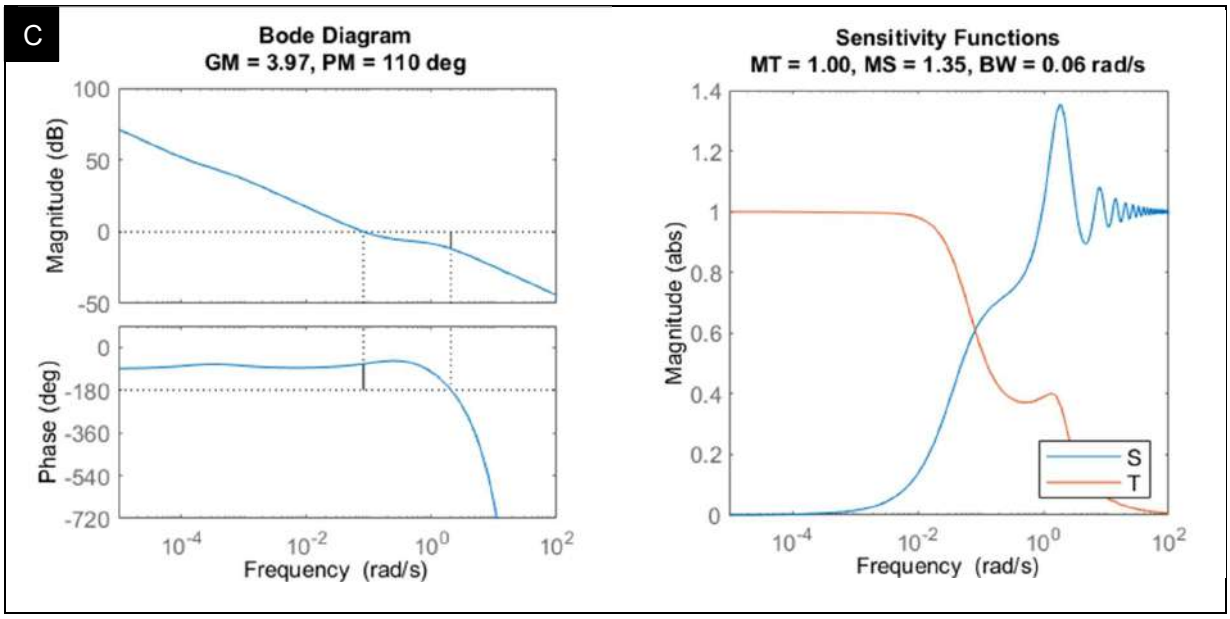

***Figure 12**: Support pump's Bode and sensitivity functions plots for the three sets of parameters. A) SSTR, B) ZN, C) TL.*

A Simulink plot comparing the closed-loop responses using the three set of parameters is shown on Figure 13. It contains a 10 bar setpoint change at time 0, as well as a unitary disturbance (mass flow) change at time 100 seconds. The discrete-time PI controllers are set with a sample time of 1 second.

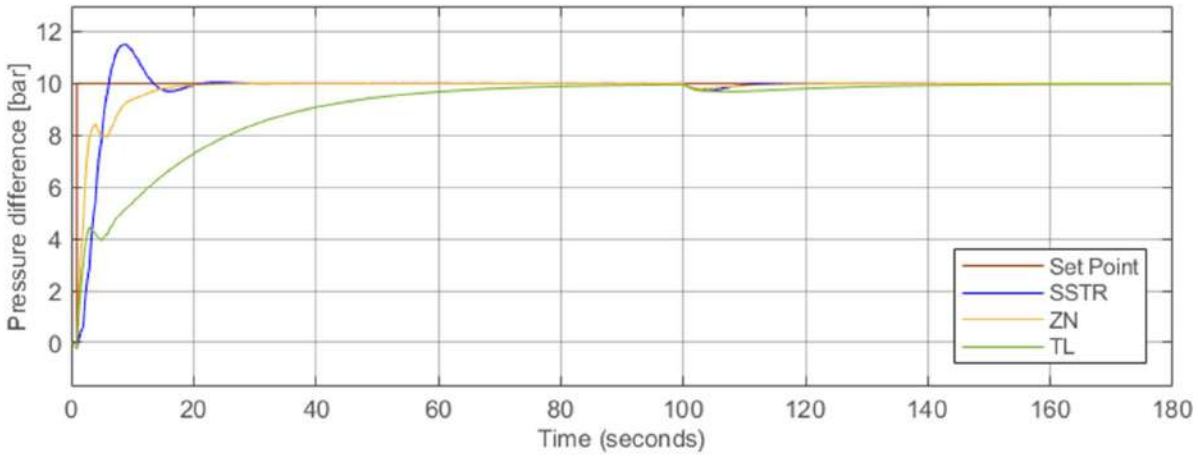

***Figure 13**: Support pump's closed-loop responses for the three set of parameters: SSTR, ZN, and TL. A setpoint change occurs at time 0 and a mass flow change, at time 100 sec. Sample time = 1 sec.*

In this case, SSTR settings provide a fast response. Nevertheless, due to its larger integral gain I, it presents an overshoot of 1.15%. When comparing it with the ZN parameters results, bandwidth values are similar, and, as Figure 13 shows, so are both settling times. The response given by the ZN settings is smoother, however, and does not present an overshoot. The third set of controller parameters, TL, has the lowest bandwidth value -up to 8 times smaller-, thus providing sluggish results. Both SSTR

and ZN settings produce very similar responses to the disturbance change, much faster than that produced by the TL parameters.

Once again, all phase margin values are greater than the specification. In respect to gain margin, SSTR's value is 40% larger than the design recommendation. All M_T and M_S results are within the specificized ranges.

All things considered, although the settings used during the Summer Semester test run provide a fast response and good disturbance rejection, Ziegler-Nichols settings also manage to accomplish these goals, while at the same time, producing smoother responses without overshoots. Robustness and stability are also guaranteed for the ZN parameters, as all values follow Seborg's design specifications. Consequently, these settings provide the overall best performance.

4.3 Throttling Valve Loop

The ultimate gain and period corresponding to the throttling valve control loop are: Kcu = 1.01, and Pu = 4 seg. Table 13 shows the controller settings. For the filter coefficient calculation, an α value of 0.2 was selected:

Set	P	I	D	N
SSTR	0.02	0.25	1.00	0.33
ZN	0.61	0.50	0.50	10.00
TL	0.45	0.11	0.63	8.00

Table 13: *Throttling valve's Summer Semester, Ziegler-Nichols and Tyreus-Luyben PID controller settings*

MATLAB's Bode and sensitivity functions' magnitude plots are presented on Figure 14:

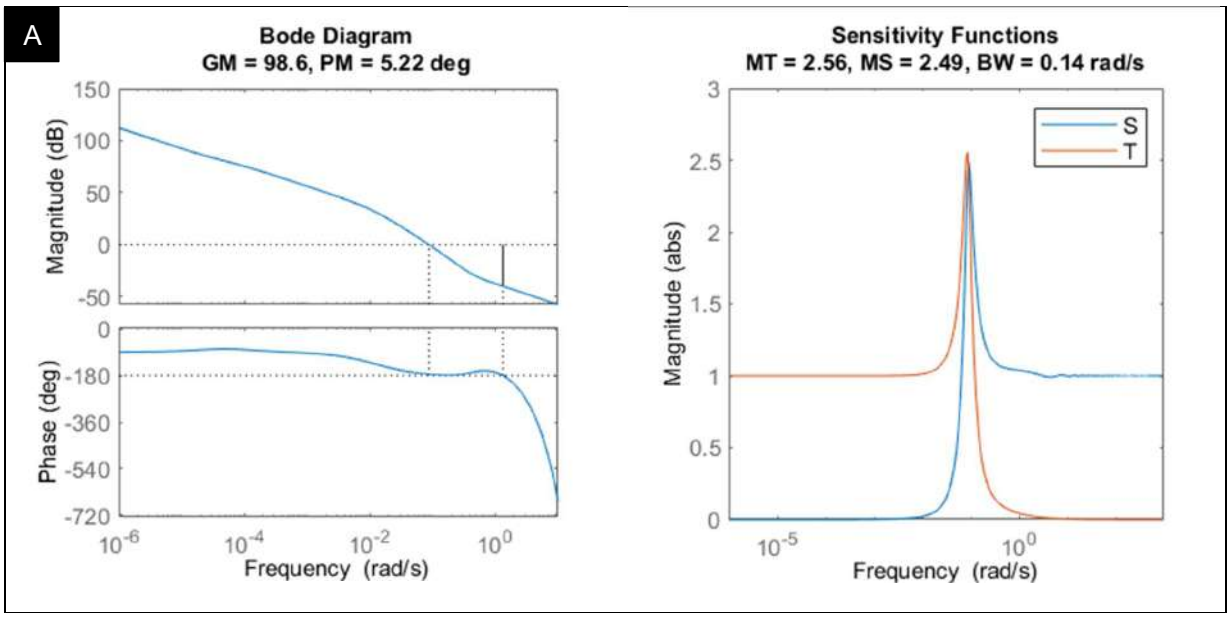

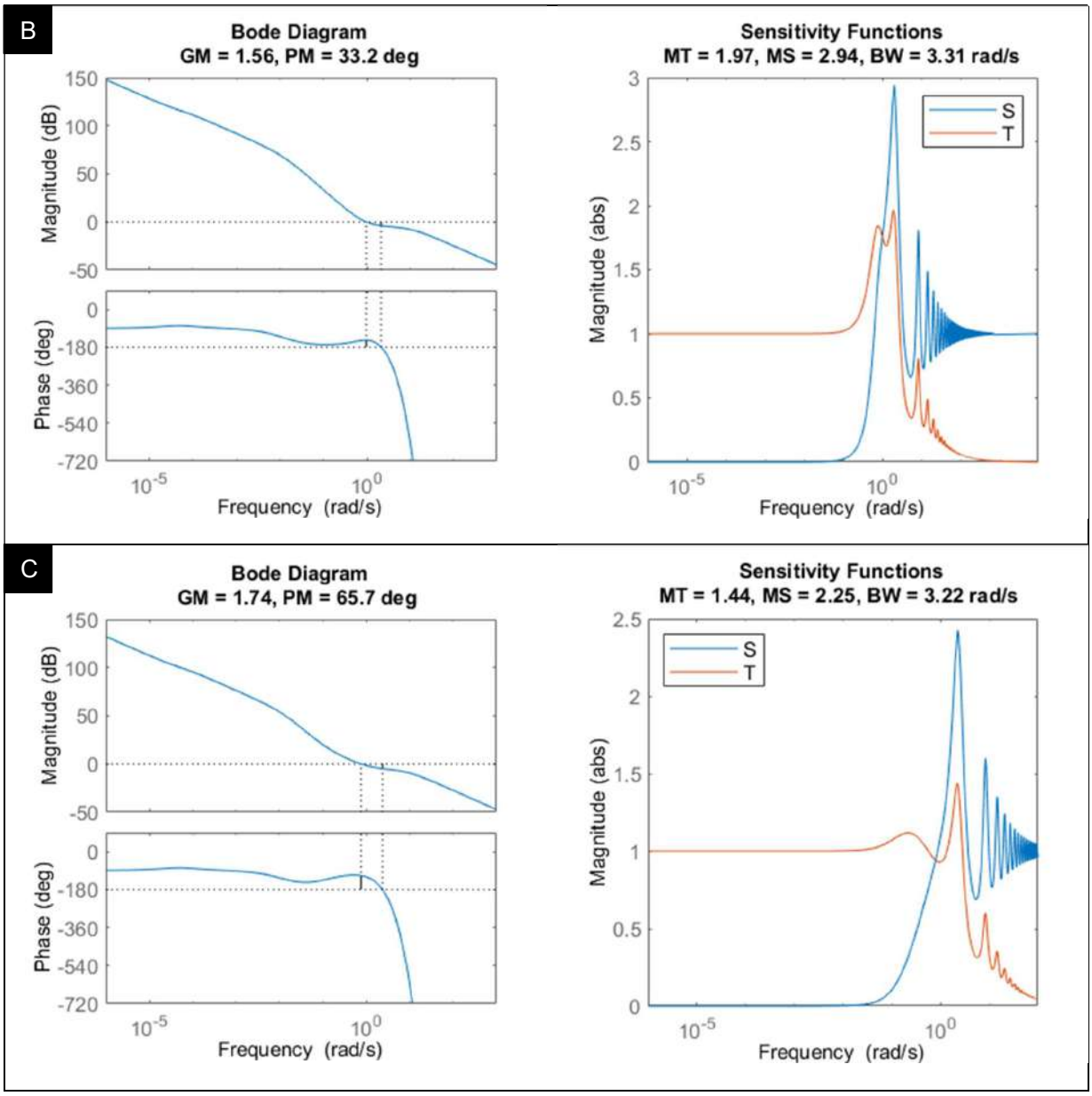

***Figure 14**: Throttling valve's Bode and sensitivity functions plots for the three sets of parameters. A) SSTR, B) ZN, C) TL.*

A Simulink plot comparing the closed-loop responses using the three set of parameters is shown on Figure 15. It contains a 10 bar setpoint change at time 0, as well as a first disturbance (inlet density) change at time 1500 seconds, and a second disturbance (mass flow) change at time 2500 seconds. The discrete-time PID controllers are set with a sample time of 1 second.

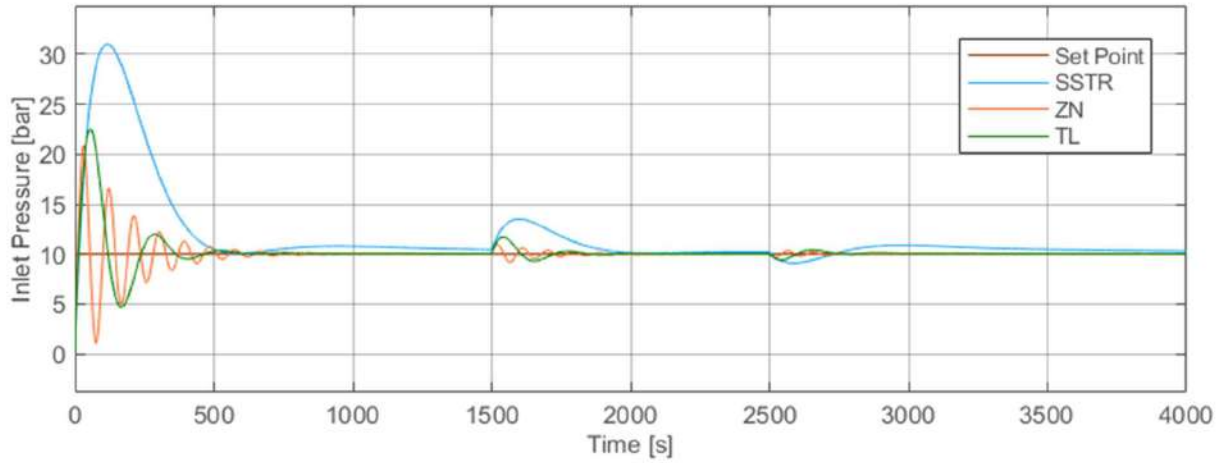

***Figure 15**: Throttling valve's closed-loop responses for the three set of parameters: SSTR, ZN, and TL. A setpoint change occurs at time 0, a density disturbance change, at time 1500 s, and a mass flow disturbance change, at time 2500 s. Sample time = 1 sec.*

Figure 15 shows that none of the three sets of parameters provide smooth setpoint responses: ZN and TL produce oscillatory, yet faster responses compared to the SSTR settings, whose overshoot is unacceptably large. Its disturbance responses are also the slowest. This is explained by its bandwidth value, which is 23 times smaller than ZN's and TL's.

The sensitivity values indicate that the SSTR and ZN settings are more aggressive than the TL parameters. In fact, according to the guidelines, they are too large. Regarding the stability analysis, ZN and TL's gain and phase margins have acceptable values. SSTR, however, present a large gain margin and a very small phase margin, both beyond the ranges of the recommendations.

Among the three sets studied, the Tyreus-Luyben PID controller parameters provide the overall best performance. Fast yet slightly oscillatory -still less than ZN's response-, stability and good disturbance rejection are achieved.

Next step is to evaluate the selected sets of parameters in each Simscape model, and compare their responses with the measured data, which was obtained using the SSTR settings.

4.4 Simscape Models Results

A summary of the optimized controller parameters is shown on Table 14.

Control Loop	P	I	D	N
Main Pump	14.70	0.60	-	-
Support Pump	14.40	0.40	-	-
Throttling Valve	0.45	0.11	0.63	8.00

***Table 14:** Final optimized controller settings*

The process transfer functions are replaced by the Simscape models, which have been already validated, and simulations are run using the optimized controller settings, as well as the setpoint data -taken from data set #2- as input.

All individual models are connected to one another in one single file: the support pump's outlet represents the main pump's inlet, while the main pump's discharge pressure is given by the throttling valve. The mass flow, which is defined in the LEWA pump, is shared through all components. Comparisons of the models' responses with the measured data are presented on Figure 16, together with a supporting plot showing a detail of the responses to a setpoint change.

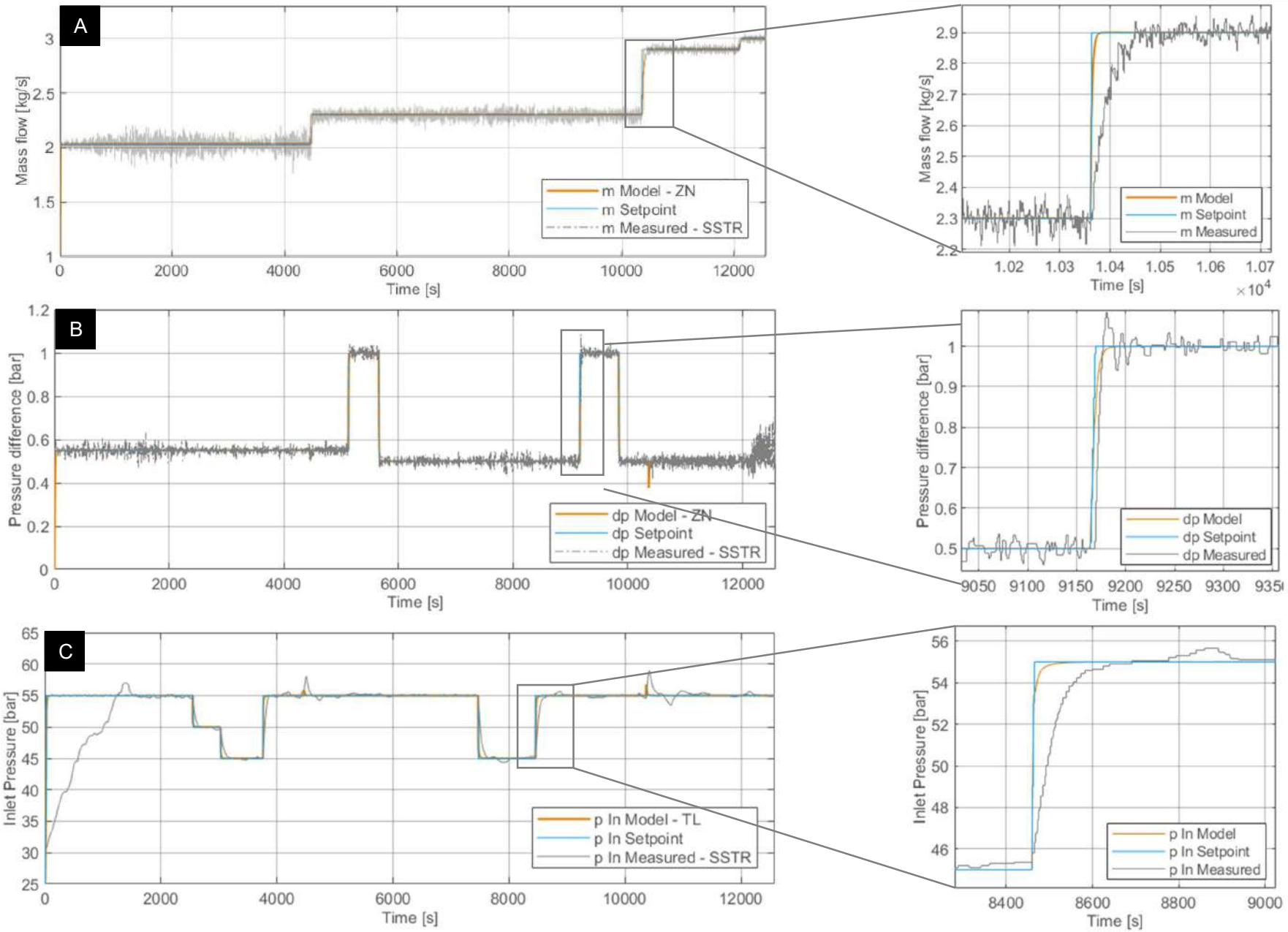

Figure 16: *Comparison of the closed-loop responses using the optimized controller settings with the measured data. A) Main pump, B) Support pump, C) Throttling Valve*

To begin with, the main pump responses comparison shows that the Ziegler-Nichols controller parameters provide the expected level of setpoint tracking. Accordingly to the previous transfer function analysis, the response to changes is smooth and does not present overshooting. The detail plot also shows that it is ~8 times faster than the measured data, and no offset occurs. It is important to consider that this data present different levels of noise, which is inherent to the measurement process and depends on the plant's instrumentation.

Regarding the support pump, it is clear when observing the detail plot that the overshoot present in the SSTR setpoint response -the measured data- is eliminated when using the ZN parameters. This result concurs with the previous analysis, as well as the fact that both set of parameters provide a similar settling time of ~20 seconds. With respect to disturbance rejection, it is possible to analyze two responses that match the mass flow setpoint changes that are shown on Figure 16-A: the first one, around time 4500 seconds, in which both the model and the measured data seem almost insensitive to the perturbation; and the second one, around time 10400 seconds. In this case, both responses present a visible reaction to the mass flow change: although the ZN settings produce a separation from the setpoint which is, in amplitude, 50% larger than that produced by the SSTR parameters, it lasts 3 times shorter (25 vs 80 seconds).

Lastly, the throttling valve's responses comparison is considered. In this case, the measured data does not contain the same level of noise as the previous cases. While the SSTR response is characterized by the overshooting and sluggishness in setpoint and disturbance changes, the Tyreus-Luyben controller settings provide smooth, and at least 10 times faster responses. In contrast with the transfer function analysis results, no visible overshoot or oscillation is produced by the optimized parameters. This could be explained by the inaccuracy between the Simscape and transfer functions models. Considering the same two responses to mass flow changes as the previous case, it is possible to assert that the TL settings achieve better disturbance rejection, both in amplitude (2 times smaller) and duration (18 times shorter), than the SSTR's.

5 Conclusions

The aim of this Thesis work was, firstly, to develop process models within the MATLAB environment for the main and support pump, as well as the throttling valve, which could simulate, for a wide range of operating conditions, the real elements that conform the bypass configuration of MoNiKa. The steps required to fulfill this goal included: selecting Simscape as the modeling tool, adapting each process block to the real components' technical characteristics, and performing simulations using two sets of measurements as input data, the second one having validation purposes. Results showed that the models, which were interconnected in a single file, provided adequate fit to the measured data within the boundaries of both test runs.

Considering that MoNiKa was conceived not only as an operating power plant, but also as a research platform, the fact that it is now possible to count with a MATLAB model of each of these components stands as a tool for future works and optimization studies.

The second objective of this work was to optimize the control system by obtaining the corresponding sets of controller settings. The optimized parameters would replace the preliminary ones, which provided conservative results. In particular, three control loops were studied, each containing one of the components whose model had been developed.

In order to achieve this purpose, a transfer function for every model had to be determined through MATLAB programming. Using the measured data as inputs and outputs, and having understood the dependencies of each process, three independent transfer functions were obtained. Although the support pump's function presented the weakiest fit to data, the overall results were satisfactory.

The Continuous Cycling Method was selected as the basis of control tuning. For each of the three loops, two sets of controller settings were calculated using the Ziegler-Nichols [15] and Tyreus-Luyben [16] tuning formulae. Sensitivity and stability results were obtained based on frequency analysis, and were compared according to the design guidelines presented by Seborg et al. [12].

The optimized PI controller parameters determined for the main pump loop (P = 14.7, I = 0.6) provided smooth, yet up to 8 times faster responses to setpoint changes than the preliminary settings. Stability values proved to follow the design recommendations.

As for the support pump loop, its optimized parameters (P = 14.4, I = 0.4) managed to eliminate the overshoot present in the response given by the preliminary settings, while maintaining its settling time, which was already acceptably short (~20 seconds). Sensitivity to mass flow changes proved to last shorter, although producing a 50% larger separation to the setpoint.

The selected PID controller parameters for the throttling valve loop (P = 0.45, I = 0.11, D = 0.63, N = 8.00) provided at least 10 times faster responses to setpoint changes than the preliminary settings. Its responses to mass flow and density perturbations were also smaller, both in amplitude and duration.

In conclusion, the three selected sets of controller parameters provided an optimized performance, both in setpoint tracking and disturbance rejection. Moreover, while avoiding excessive or aggressive control action, they proved to follow the stability and sensitivity guidelines, with the exception of the phase margin values, which were conservatively above the recommendation: up to 99°, vs 30°, which is the lower value indicated before becoming instable.

6 References

[1] Van Nguyen, M., Arason, S., Gissurarson M. and Pálsson, P.G. Uses of geothermal energy in food and agriculture – Opportunities for developing countries. Rome, FAO. 2015.

[2] Herfurth, S., Kuhn, D., Wiemer, H.-J.; Performance Optimization of ORC Power Plants. Proceedings World Geothermal Congress, 2015.

[3] Kuhn, D.: Modular Low Temperature Cycle Karlsruhe. Internet: www.monika.kit.edu/english

[4] Vetter, C.; Wiemer, H.-J.; Kuhn, D.: Comparison of sub- and supercritical Organic Rankine Cycles for power generation from low-temperature/low-enthalpy geothermal wells, considering specific net power output and efficiency. Applied Thermal Engineering 51, 2013. 1-2, S. 871–879.

[5] Gardella, L.: Analysis and Evaluation of MoNiKa's first results in bypass configuration. Master Thesis, ITES, Karlsruhe Institute of Technology, 2020.

[6] Grundfos. 2019. Datasheet product CRN 20-4 A-FGJ-A-E-HQQE. Manufacturer document.

[7] Lewa GmbH. 2019. Technisches Datenblatt. Manufacturer document.

[8] Vetec Ventiltechnik GmbH. 2014. Technisches Datenblatt 73.7. Manufacturer document.

[9] The MathWorks, Inc. 2020. Simscape.

[10] REFPROP. Reference Fluid Thermodynamic and Transport Properties Database. National Institute of Standards and Technology, 2018.

[11] The MathWorks, Inc. 2020. MATLAB.

[12] Seborg, Dale E.; Edgar, Thomas F.; Mellichamp, Duncan A., Process dynamics and control. 2nd Edition. Wiley, 2003.

[13] Siemens Energy, 2020. SPPA-T3000 Control System

[14] Siemens Energy, 2020. Continuous controller with setpoint adjuster. CCTRL ID 303.

[15] Ziegler, J. G. and N. B. Nichols, Optimum Settings for Automatic Controllers, Trans. ASME, 64, 759, 1942.

[16] Luyben, W. L. and M. L. Luyben, Essentials of Process Control, McGraw Hill, New York, 1997.

7 List of Figures

8 List of Tables

9 Appendix

9.1 Data set #1: Measurements collected on the Winter Semester test run (23.01.2020)

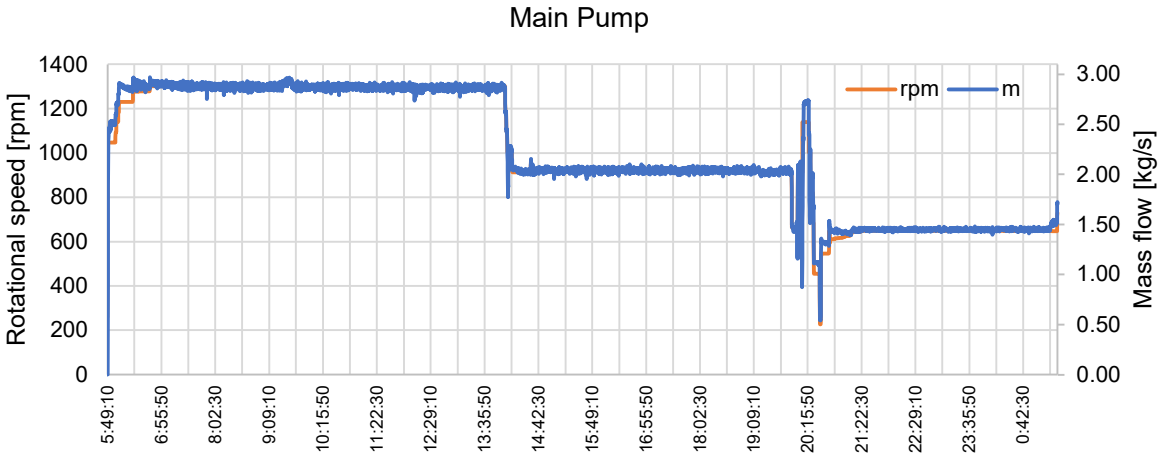

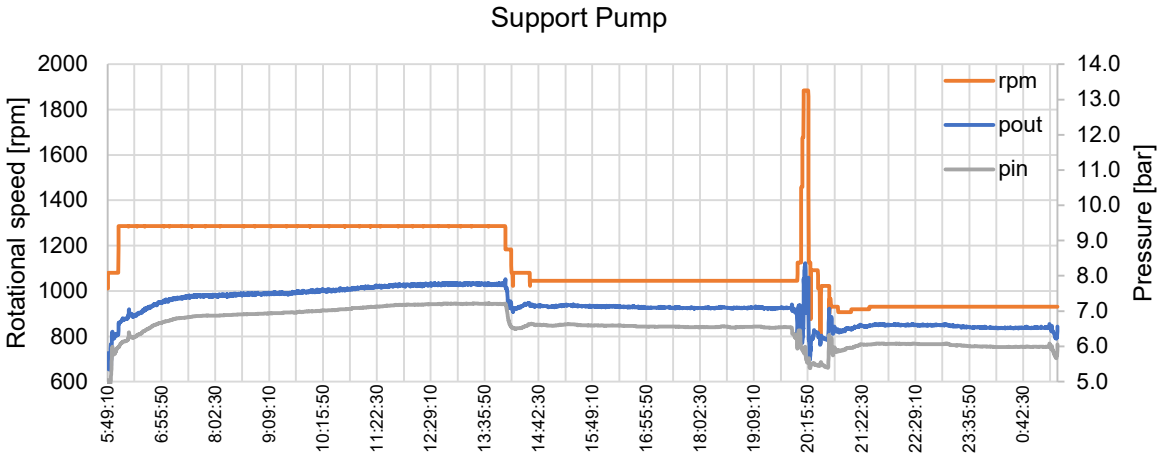

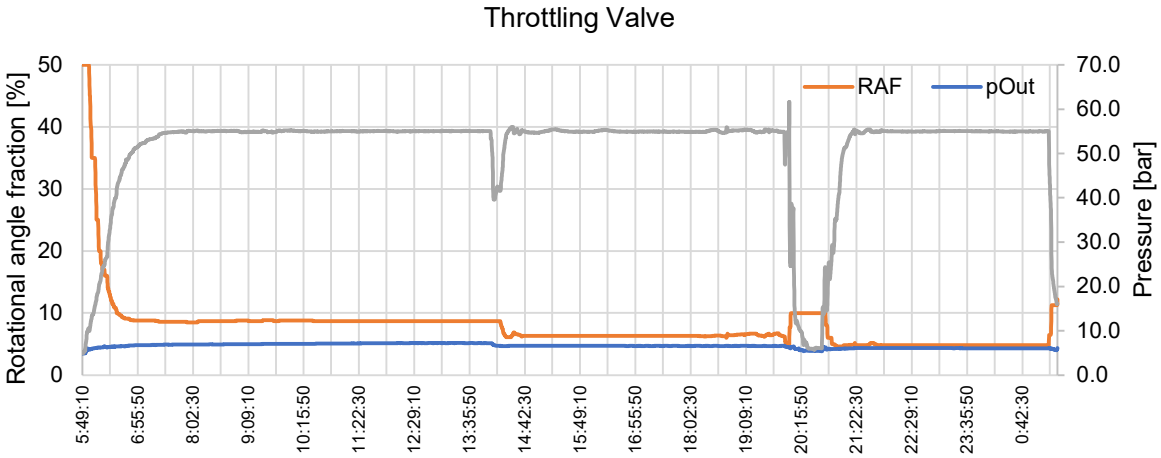

9.2 Data set #2: Measurements collected on the Summer Semester test run (02.07.2020)

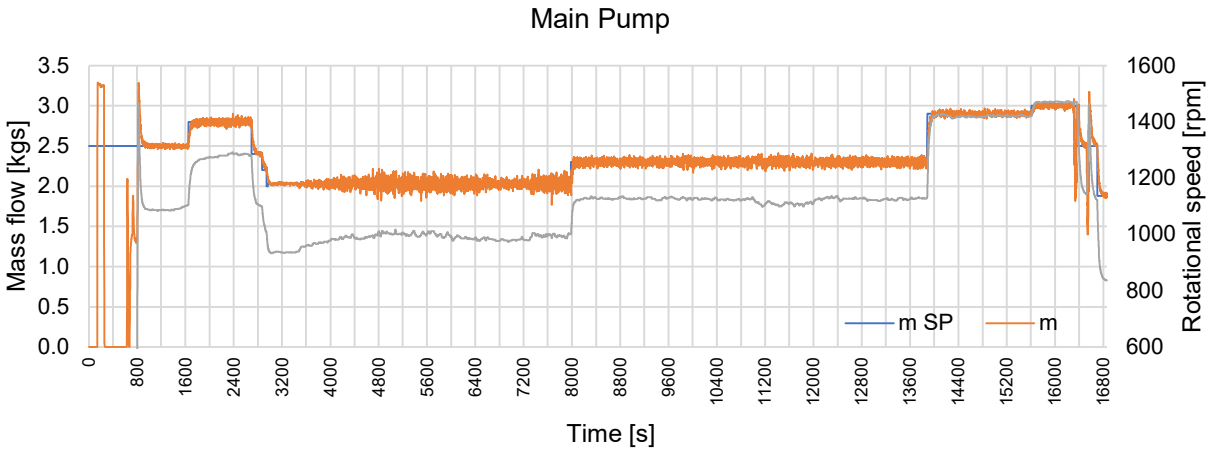

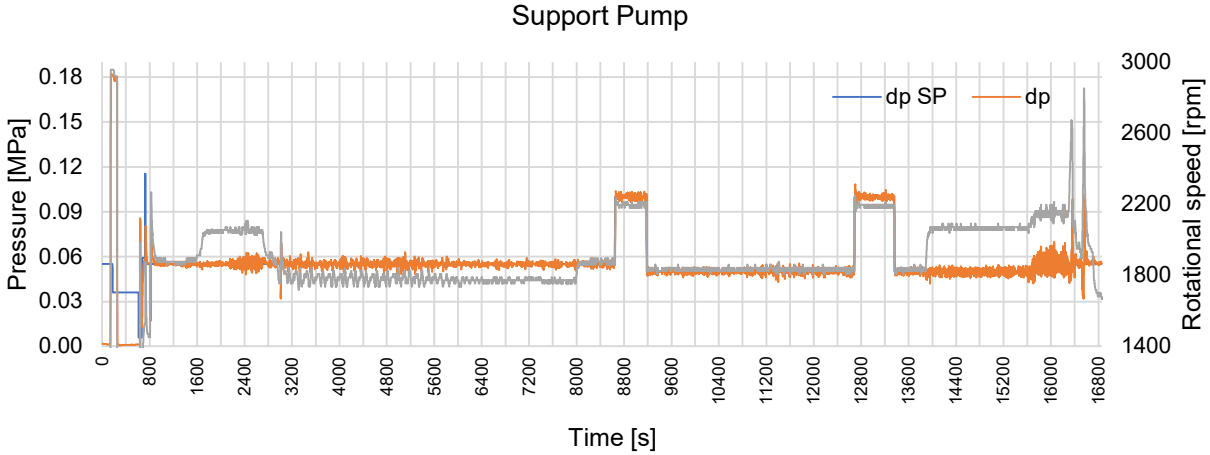

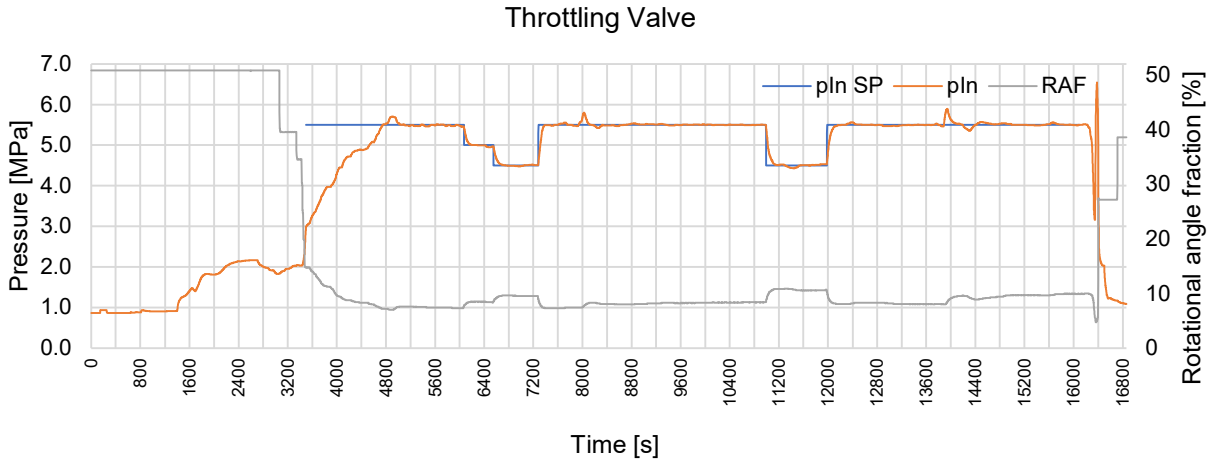

9.3 Process models: Simscape interface arrangements

Main Pump:

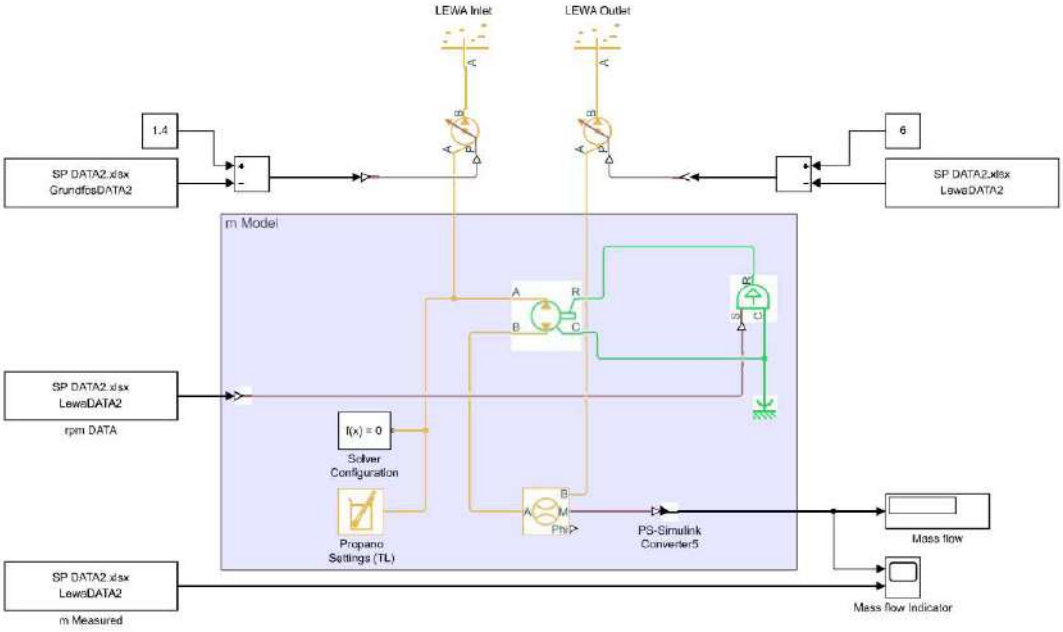

Support Pump:

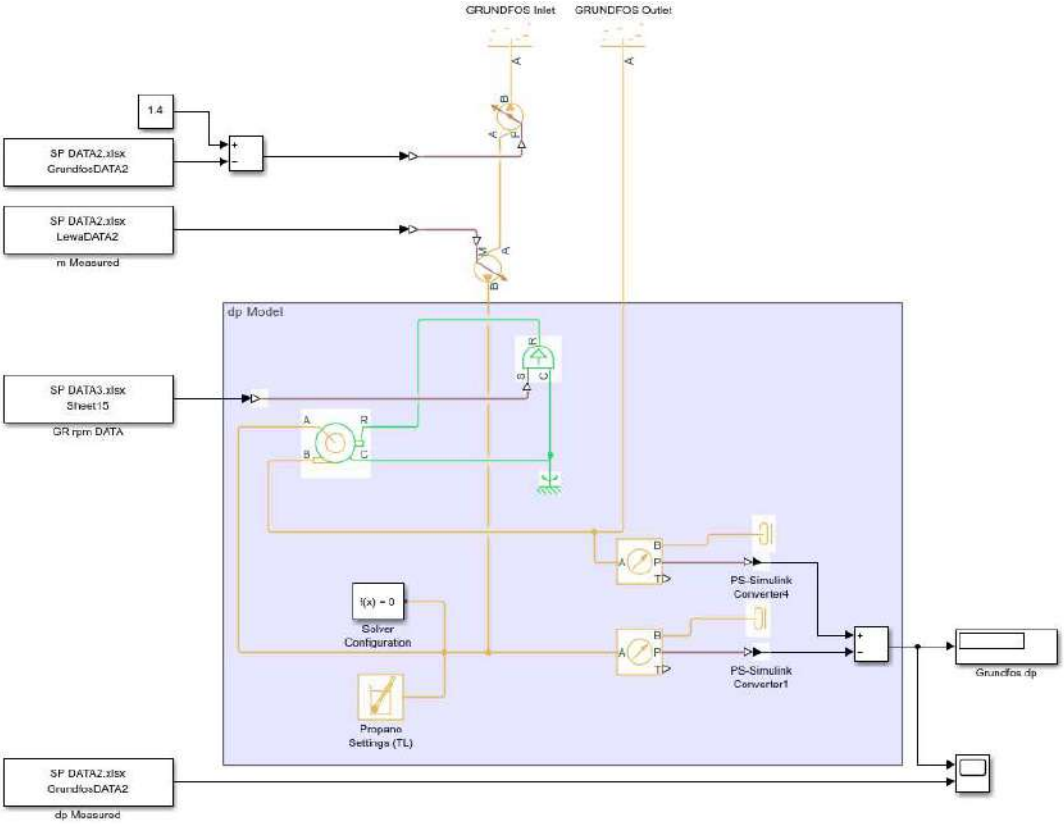

Throttling Valve:

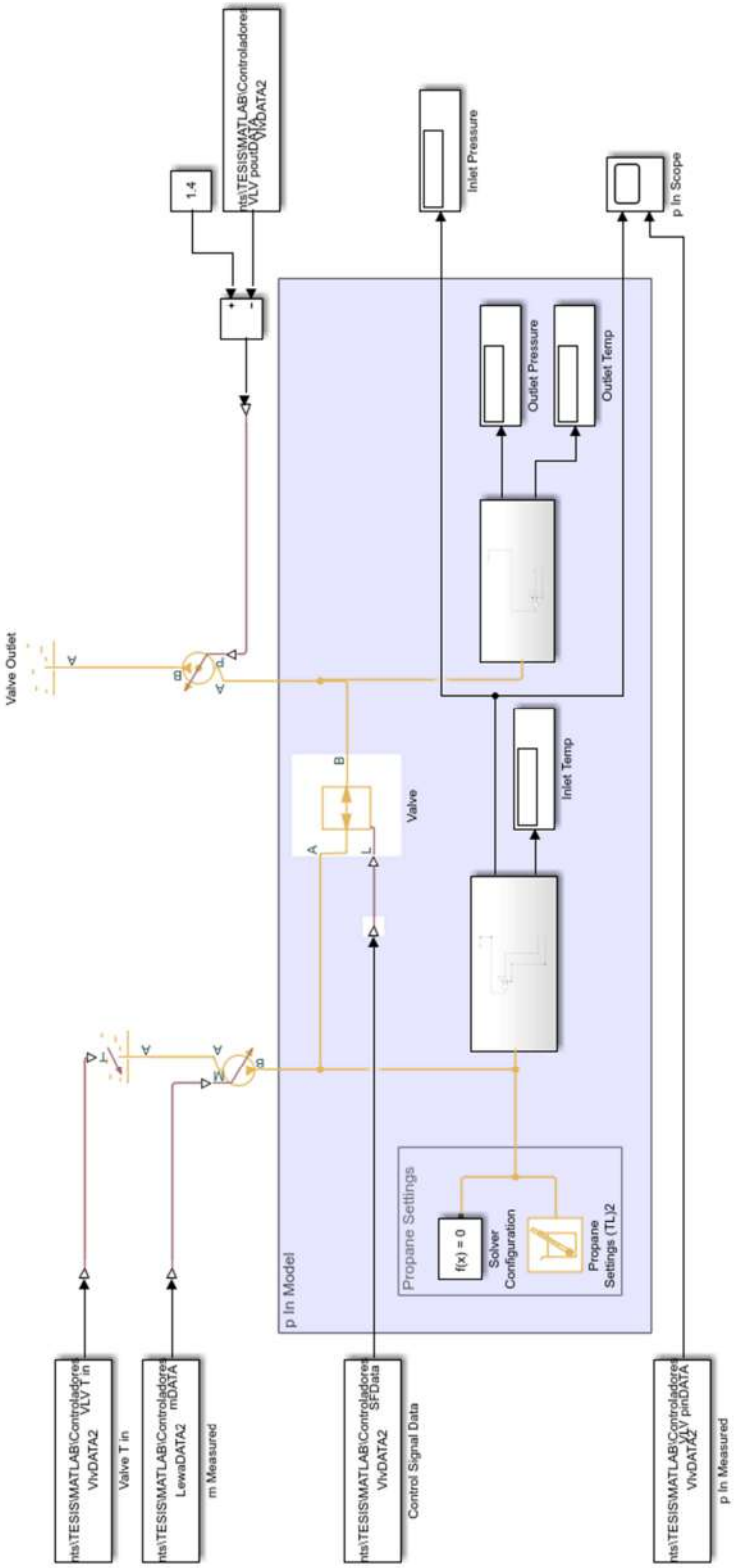

Control System:

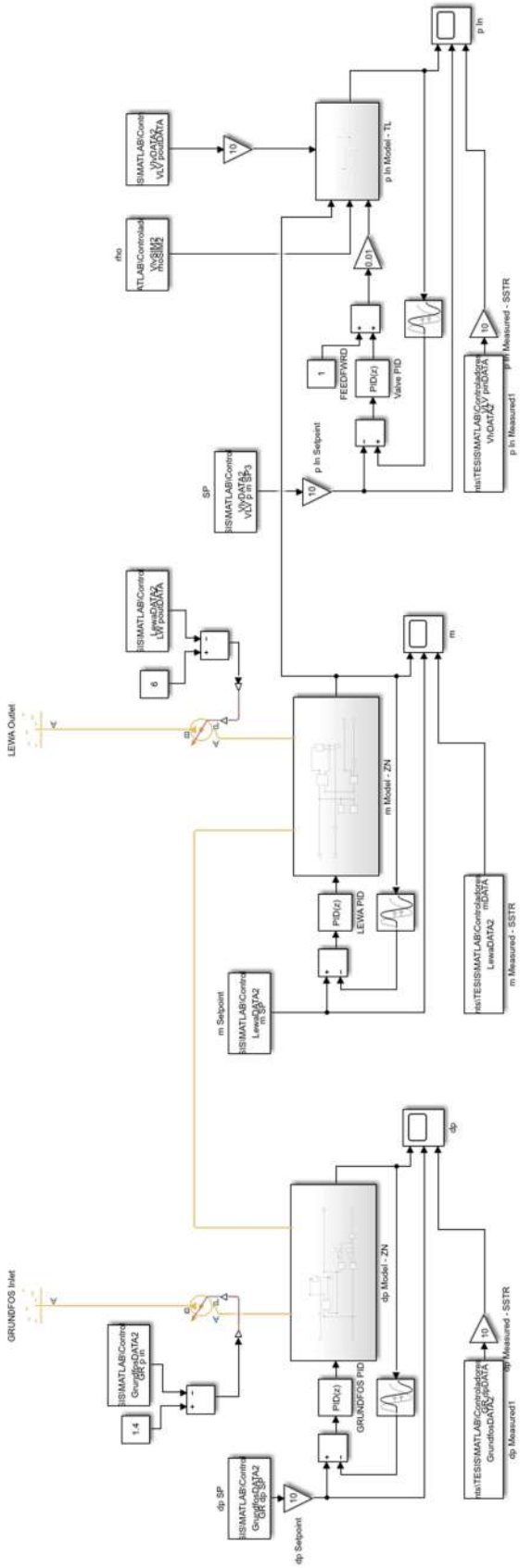

9.4 MATLAB Programs

9.4.1 Transfer functions calculation

By changing the input and output data, the following code can be used to calculate the transfer function of any of the main components:

```
clc;
clear all;

%% Input and output data

time=xlsread('DataTF2', 'VlvDATA2', 'a1850:a12582');
input1=xlsread('DataTF2', 'VlvDATA2', 'p1850:p12582');
input2=xlsread('DataTF2', 'LewaDATA2', 'd1850:d12582');
input3=xlsread('DataTF2', 'VlvDATA2', 'r1850:r12582');
output=xlsread('DataTF2', 'VlvDATA2', 'n1850:n12582');

ts = time(2)-time(1); % assuming uniform time grid
data = iddata(output, [input1  input2  input3] , ts);

%% Laplace Variable

s = tf('s');

%% Transfer function from data

np=2;
nz=1;
iodelay = NaN;

sys = tfest(data,np,nz,iodelay)
tr_zpk = zpk(sys);

%% Zeros and poles

Z = tr_zpk.Z{1};
P = tr_zpk.P{1};
K = tr_zpk.K;

figure('Name','pzmap');
pzmap(tr_zpk);

%% Impulse Response

figure('Name','Impulse');
[ y_i , t_i ] = impulse(tr_zpk);
Impulse_info = lsiminfo(y_i,t_i,0);

%% Unitary Step Response

figure('Name','STEP');
step(tr_zpk);
Step_info = stepinfo(tr_zpk);
```

9.4.2 Stability and sensitivity analysis

Main Pump:

```
clc;
clear all;

%% Laplace Variable

s = tf('s');

%% Transfer functions

% Controller settings
% Kc = 1;
Kc = 14.7;
Ti = 0.6;

% Process
sys = tf( [0.133, 0.0004164], [1, 63.87, 0.2037] );
Gc = Kc + ((Kc * Ti)/ s );
% Gc = Kc;
Gv = 14.7;
Gp = sys;
Gme = exp(-1*s);
Gol = Gc*Gv*Gp*Gme;

%% Bode

figure('Name','Bode')
bode(Gp,Gol)
legend('Gp','Gol')

figure('Name','Margin Gol')
margin(Gol)
[Gm,Pm,Wcg,Wcp] = margin(Gol)


%% Sensitivity

G = Gv*Gp*Gme ;
S = 1 / ( 1 + (Gc*G) ) ;
T = (Gc*G) / ( 1 + (Gc*G) ) ;

figure('Name','Sensitivity')
bodemag(S,T)
legend('S','T')

BW = bandwidth(Gol)
```

Support Pump:

```
clc;
clear all;

%% Laplace Variable

s = tf('s');

%% Transfer Functions

% Controller Parameters
% Kc = 1.27;
Kc = 14.4;
Ti = 0.4;

% Process
sys = tf( [0.0001339, 3.192e-08] , [1, 1.252, 0.0005812] );
Gc = Kc + ((Kc * Ti)/ s );
% Gc = Kc;
Gv = 45;
Gp = sys;
Gme = 10*exp(-1*s);
Km = 10;
Gol = Gc*Gv*Gp*Gme;

%% Bode

figure('Name','Bode')
bode(Gp,Gol)
legend('Gp','Gol')

figure('Name','Margin Gol')
margin(Gol)
[Gm,Pm,Wcg,Wcp] = margin(Gol)

%% Sensitivity

G = Gv*Gp*Gme ;
S = 1 / ( 1 + (Gc*G) ) ;
T = (Gc*Gv*Gp*Km) / ( 1 + (Gc*G) ) ;

figure('Name','Sensitivity')
bodemag(S,T)
legend('S','T')

wbw = bandwidth(Gol)
```

Throttling Valve:

```
clc;
clear all;

%% Laplace Variable

s = tf('s');

%% Transfer functions

% Controller parameters
% Kc = 1;
Kc = 0.45;
Ti = 0.11;
Td = 0.63;
N = 8;

% Process
sys = tf( [ -0.1587, - 6.243e-06 ] , [ 1, 0.01219, 7.494e-07 ] );
Gc = Kc + ((Kc * Ti)/ s )  +  ( (Kc*Td) / ((1/N) + (1/s)) ) ;
% Gc = Kc;
Km = 10;
Gv = 1;
Gp = sys;
Gme = 10*exp(-1*s);
G = Gv*Gp*Gme ;
Gol = G*( (1/55) - Gc );

%% Bode

figure('Name','Bode')
bode(Gp,Gol)
legend('Gp','Gol')

figure('Name','Margin Gol')
margin(Gol)
[Gm,Pm,Wcg,Wcp] = margin(Gol)

%% Sensitivity

S = 1 / ( 1 - (Gc*G) ) ;
T = (-1*Gc*Gv*Gp*Km) / ( 1 - (Gc*G) );

figure('Name','Sensitivity')
bodemag(S,T)
legend('S','T')

wbw = bandwidth(Gol)
```